Electronic Suplementary Information to

Mechanistic study of carboxylic acid and phosphate esters cleavage by oximate metal complexes surpassing the reactivity of highly basic free oximate anions

José Carlos Lugo-González, Paola Gomez-Tagle*, Marcos Flores-Alamo, Anatoly K. Yatsimirsky*

Universidad Nacional Autónoma de México, Facultad de Química, 04510, Mexico City, México.

E-mail: pao@unam.mx; iatsimirski46@comunidad.unam.mx

Fax: +52 55 56162010;

Tel: +52 55 56223813

Supporting Information

Table of contents

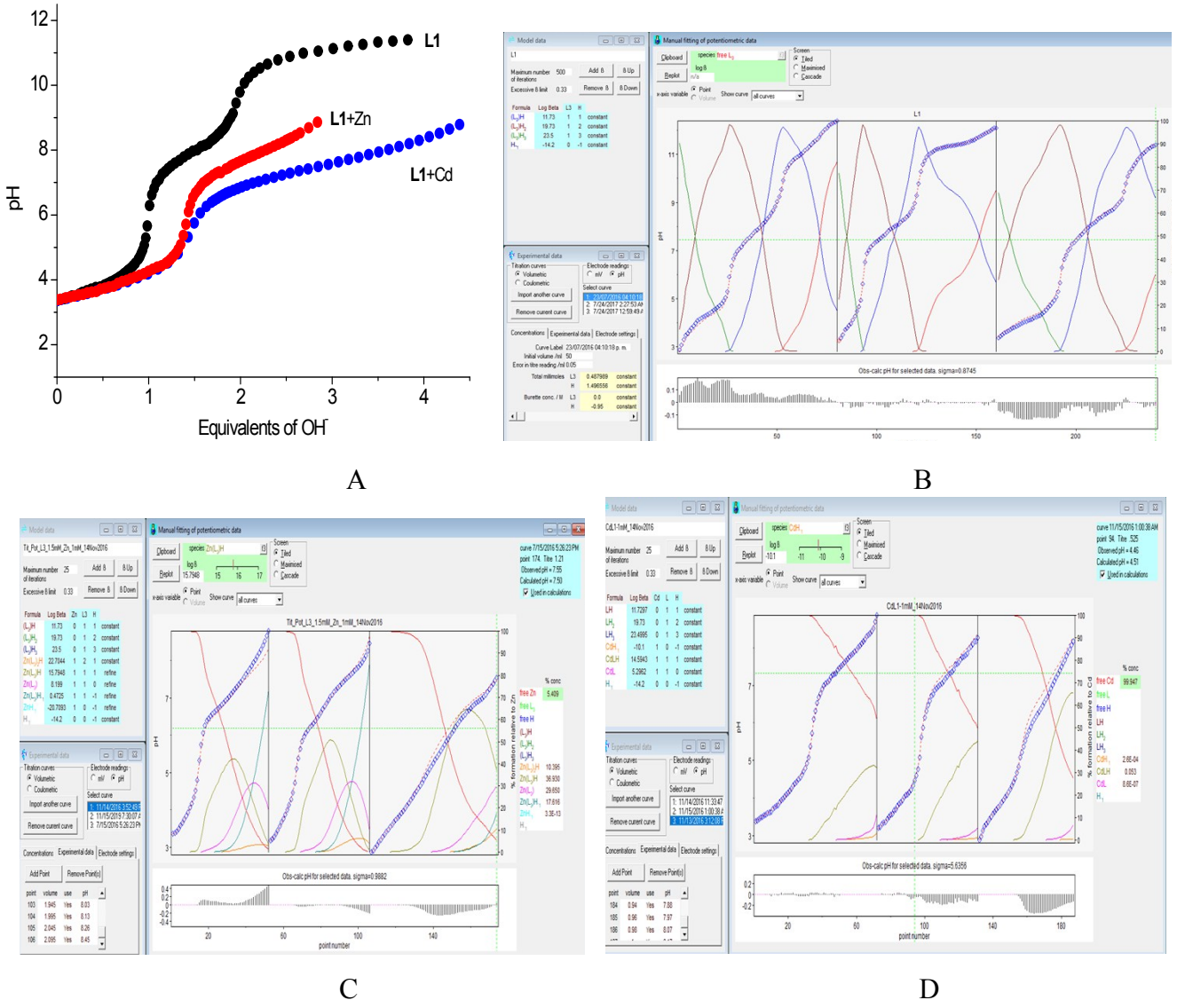

Fig. 1S. Acid-base titration curves of **L1** and their mixtures with Zn(II) and Cd(II) at 25°C and ionic strength 0.1 M. A) Titration curves of free **L1**= 1mM (black circles), **L1**= 1.3 mM and Zn(II) = 1 mM (red circles) and **L1**= 1.3 mM and Cd(II) = 1 mM (blue circles). B) Fitting of free **L1** titrations curves at 1 mM, 2 mM and 10 mM. C) Fitting of Zn(II) and **L1** mixtures titration curves at 1mM, 2 mM and 10 mM. D) Fitting of Cd(II) and **L1** mixtures titration curves at 1mM, 2 mM and 10 mM.

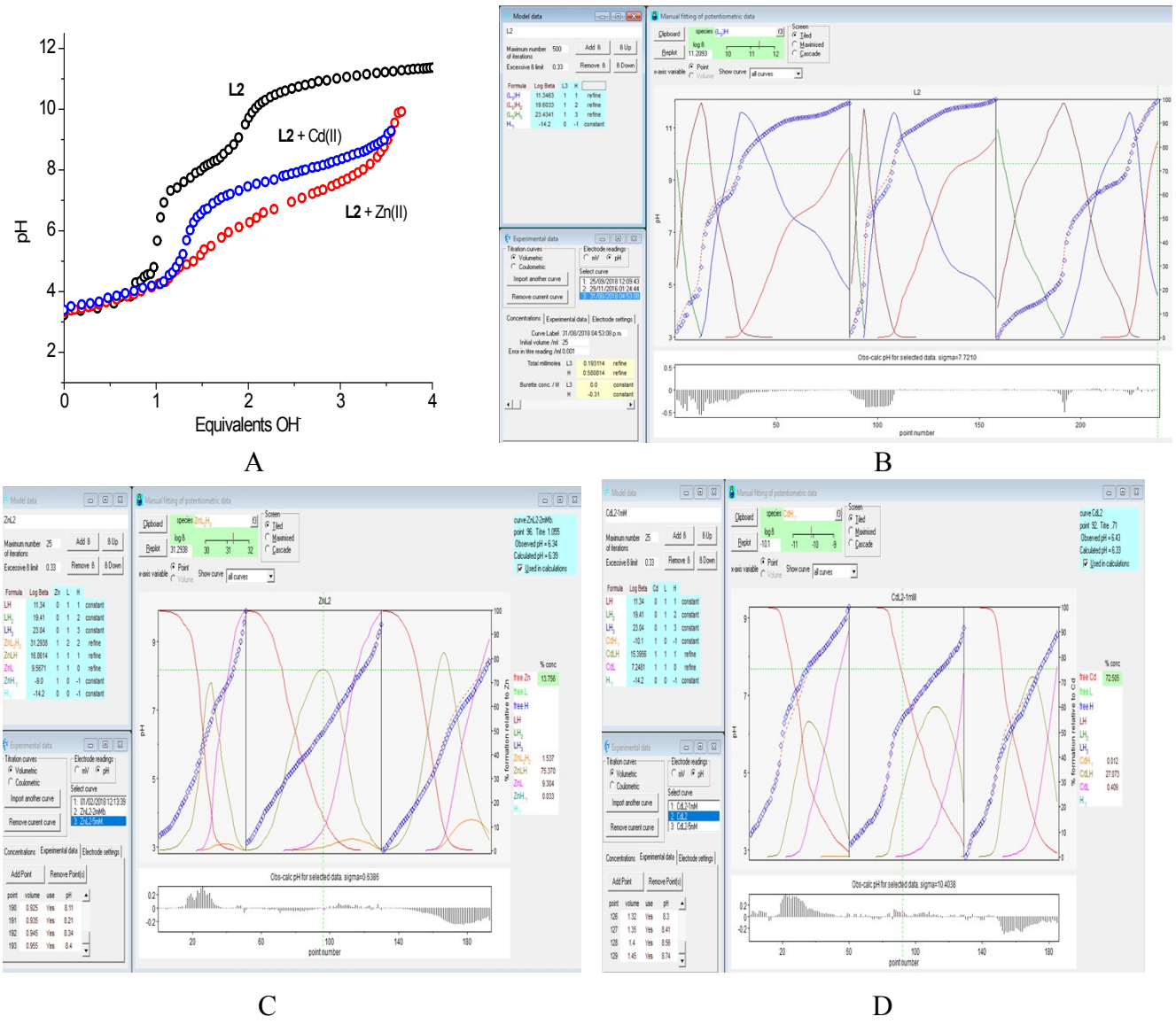

Fig. 2S. Acid-base titration curves of **L2** and their mixtures with Zn(II) and Cd(II) at 25°C and ionic strength 0.1 M. A) Titration curves of free **L2**= 1mM (black circles), **L2**= 1.3 mM and Zn(II) = 1 mM (red circles) and **L2** = 1.3 mM and Cd(II) = 1 mM (blue circles). B) Fitting of free **L2** titrations curves at 1 mM, 2 mM and 10 mM. C) Fitting of Zn(II) and **L2** mixtures titration curves at 1mM, 2 mM and 10 mM. D) Fitting of Cd(II) and **L2** mixtures titration curves at 1mM, 2 mM and 10 mM.

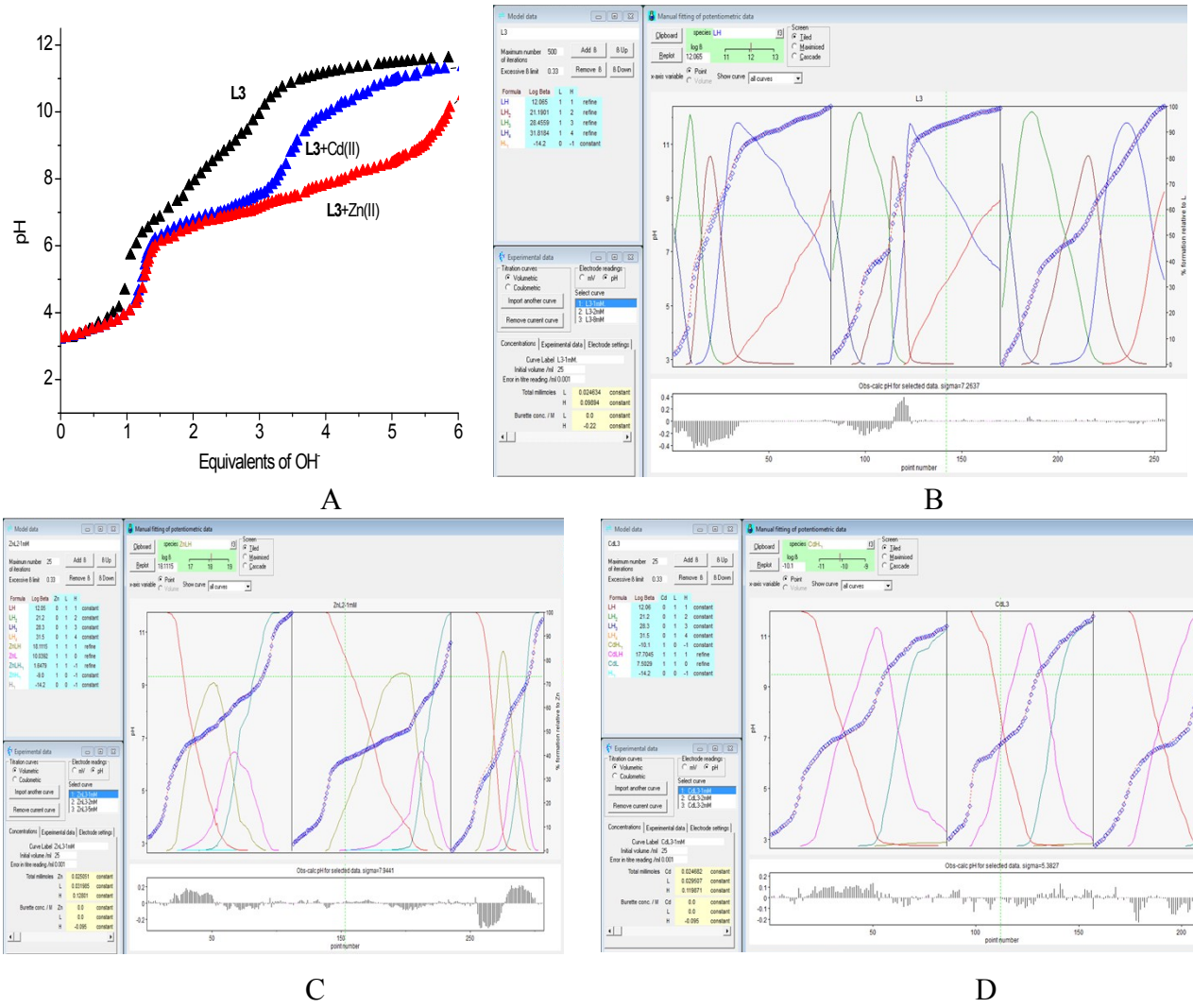

Fig. 3S. Acid-base titration curves of **L3** and their mixtures with Zn(II) and Cd(II) at 25°C and ionic strength 0.1 M. A) Titration curves of free **L3=** 1mM (black circles), **L3** = 1.3 mM and Zn(II) = 1 mM (red circles) and **L3** = 1.3 mM and Cd(II) = 1 mM (blue circles). B) Fitting of free **L3** titrations curves at 1 mM, 2 mM and 10 mM. C) Fitting of Zn(II) and **L3** mixtures titration curves at 1mM, 2 mM and 10 mM. D) Fitting of Cd(II) and **L3** mixtures titration curves at 1mM, 2 mM and 10 mM.

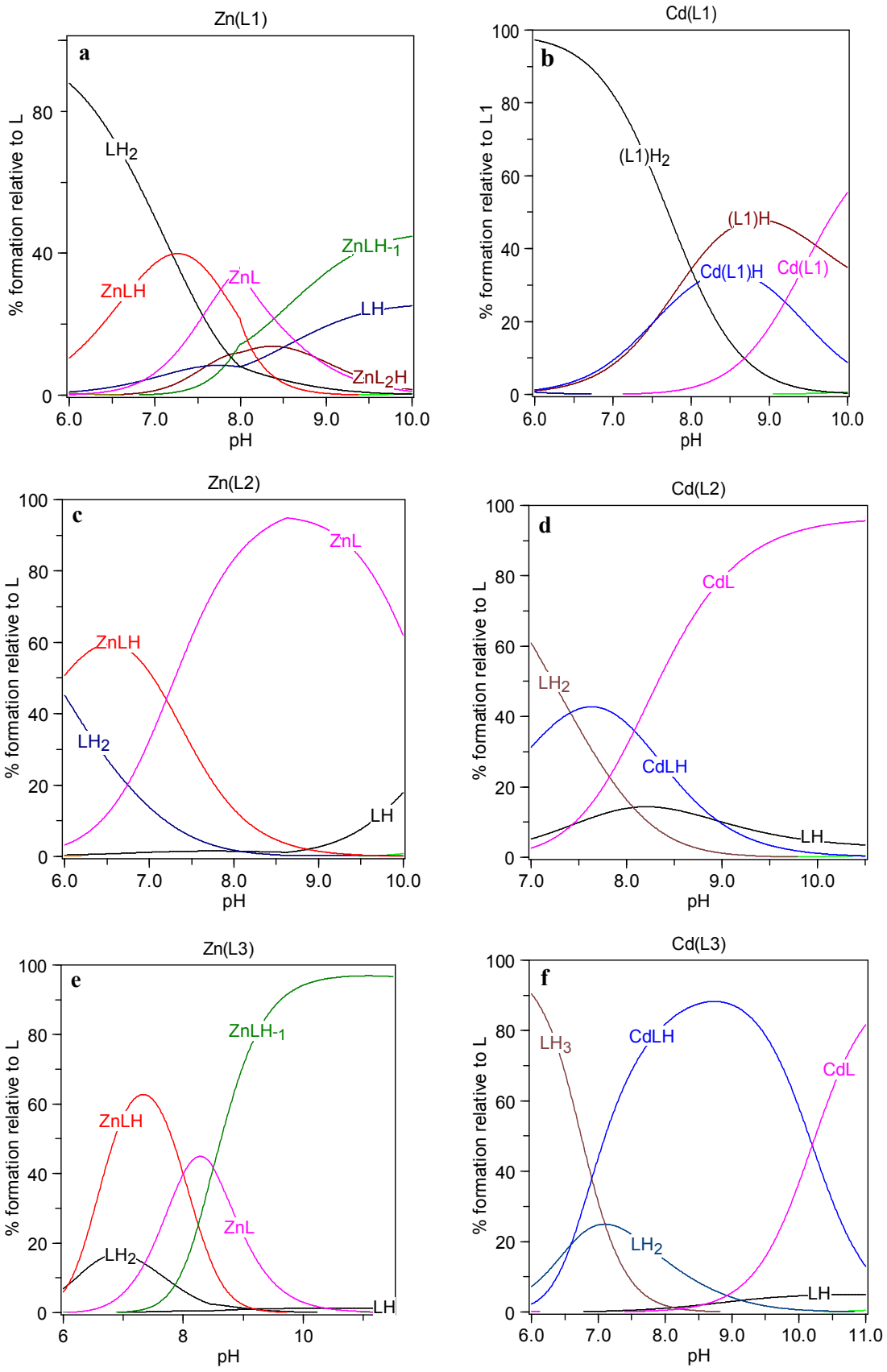
Zn(L1)
a
% formation relative to L
LH2
ZnLH
ZnL
ZnLH-1
LH
ZnL2H
pH
Cd(L1)
b
% formation relative to L1
(L1)H2
(L1)H
Cd(L1)H
Cd(L1)
pH
Zn(L2)
c
% formation relative to L
ZnL
ZnLH
LH2
LH
pH
Cd(L2)
d
% formation relative to L
CdL
LH2
CdLH
LH
pH
Zn(L3)
e
% formation relative to L
ZnLH-1
ZnLH
ZnL
LH2
LH
pH
Cd(L3)
f
% formation relative to L
LH3
CdLH
CdL
LH2
LH
pH

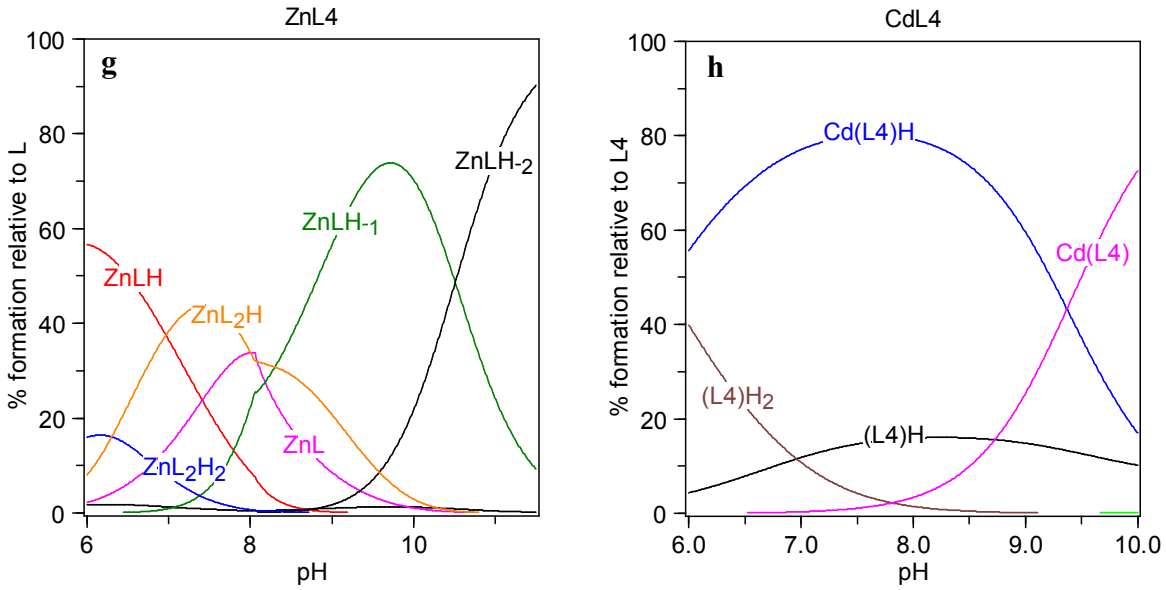

Figure 4S. Species distribution diagrams for equimolar mixtures of 1.0 mM ligands **L1-L4** with Zn(II) and Cd(II) generated by the Hyss program with the equilibrium constants from Table 1. a = **L1** and Zn(II), b = **L1** and Cd(II), c = **L2** and Zn(II), d = **L2** and Cd(II), e = **L3** and Zn(II), f = **L3** and Cd(II), g = **L4** and Zn(II) and, h = **L4** and Cd(II).

The species distribution diagrams for each system at 1.0 mM both total metal and ligand shown in Figure 4S are representative for conditions of potentiometric titrations (Figures 1S, 2S and 3S). The principal difference with species distributions in the conditions of kinetic studies (Figures 3 and 4, Main Text) is a significant contribution of the bis-complex $[Zn(H\mathbf{L4})_2]^{2+}$ to the speciation.

Acid-base and coordination properties of L1-L4 (comments to Table 1)

All free ligands undergo acid dissociation of the oxime group (reaction 1) and protonation of amine donor groups (reactions 2-4). The pK_a values of oxime groups lie between 11.30 and 12.1 in the range typical for aliphatic oximes. In the presence of metal ions the predominant species in neutral and weakly acid solutions are 1:1 complexes $[M(\mathbf{HL})]^{2+}$ with stability constants for tridentate neutral ligands **2** and **4** of the same order of magnitude as those for the complexes with parent bidentate 2-picolylamine ligand (logK = 5.3 for Zn(II) and 4.12 for Cd(II),[1] indicating a weak metal binding to neutral low basic oxime group. This agrees with the longest Cd-N bond in the complex $Cd(H\mathbf{L4})_2(NO_3)_2$ with oxime nitrogen among all three Cd-N bonds: Cd-N_{Py} =2.336, Cd-N_{NH} = 2.412, Cd-N_{NOx} = 2.421 Å. The stability of $[M(H\mathbf{L1})]^{2+}$ is smaller due to the presence of a six-membered 2-pyridyne 2'-ethylamino chelate ring.[2,3] This effect is not seen with **L2** involving a six-membered cycle

with oxime probably because of mentioned above weak coordination of the oxime group. The complexes $[M(H\mathbf{L3})]^{2+}$ have the greater stability, expected due to the presence of an additional 6-methylamine donor. In all cases, the stabilities of cadmium(II) complexes are lower than those of the zinc(II) complexes in agreement with more electrophilic character of Zn(II) and relative stabilities of their 2-picolylamine complexes (see above). The bis-complexes $[M(HL)_2]$ are observed only with L2 and **L4** (Table 1) and with Zn(II). They contribute insignificantly to total speciation in diluted solutions employed in the kinetic studies.

The speciation of Zn(II) complexes in basic solutions is complicated by concomitant dissociation of coordinated water affording mixed hydroxo complexes. The assignment was performed on basis of kinetic results taking advantage of very strong difference in reactivity of coordinated hydroxide and the oximate group. The deprotonation sequence (reactions 7 - 10) is specific for a given metal complex. In $[Zn(H\mathbf{L3})]^{2+}$ and $[Zn(H\mathbf{L4})]^{2+}$ water deprotonates before the oxime, $[Zn(H\mathbf{L3})]^{2+} \rightarrow [Zn(H\mathbf{L3})(OH^-)]^{+} \rightarrow [Zn(\mathbf{L3}^-)(OH^-)]$. With **L1** the deprotonation sequence is the opposite: $[Zn(H\mathbf{L1})]^{2+} \rightarrow [Zn(\mathbf{L1}^-)]^{+} \rightarrow [Zn(\mathbf{L1}^-)(OH^-)]$. Such inversion in the deprotonation sequence may occur because of the lower pK_a of oxime group in $[Zn(H\mathbf{L1})]^{2+}$ while the pK_a of coordinated water molecules are located in a rather narrow interval between 7.4 and 8.4 within the range typical for amine complexes of Zn(II).[3] Finally the complex $[Zn(H\mathbf{L2})]^{2+}$ undergoes deprotonation only of the oxime function yielding $[Zn(\mathbf{L2})]^{+}$ without the formation of any hydroxo species.

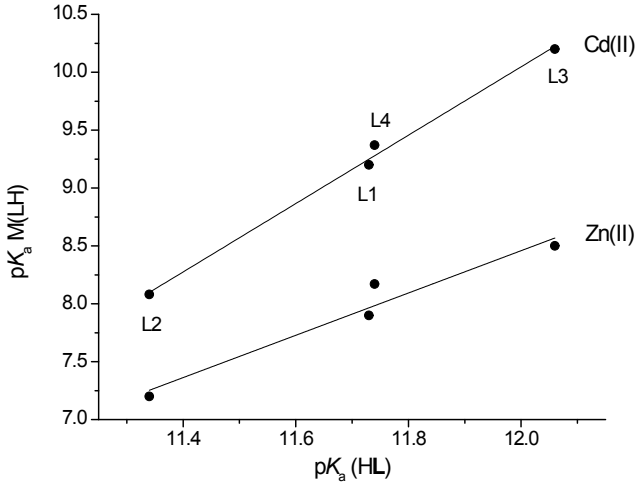

Fig. 5S. pK_a (MH**L**) vs pK_a(H**L**) for Zn^{2+} and Cd^{2+} complexes with ligands **L1** - **L4**.

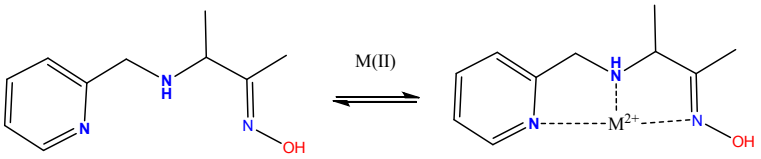

L4 + Cd(II) **L4** + Zn(II)

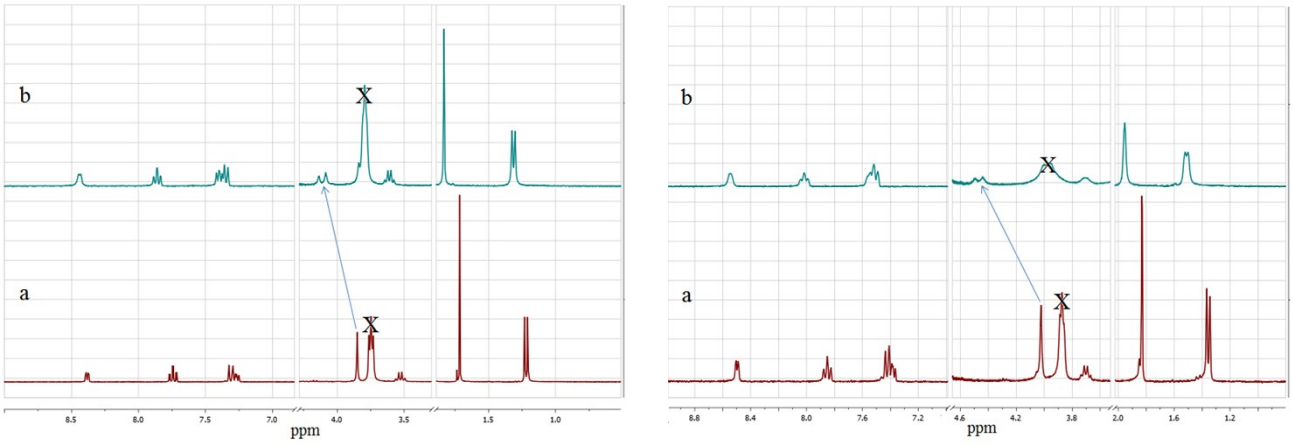

Fig. 6S. ^{1}H NMR (300 MHz) spectra of 0.01 M free ligand **L4** (a) and the 1:1 mixture of **L4** and M(II) (b) at pH 7. The crossed peak belongs to MOPS buffer; signals of water and other signals of MOPS are eliminated.

The complex formation was confirmed also by ^{1}H NMR. A typical example is shown in Figure 6S, which compare the spectra of free ligand **L4** and the 1:1 mixtures of **L4** with Zn(II) and Cd(II) under conditions when the principal species is the $M(HL)^{2+}$ complex. The characteristic changes in the signals of protons of **L4** induced by the complexation involve downfield shifts of all signals due to the deshielding effect of the positive charge of the metal ion, which confirms coordination with all three nitrogens, and the transformation of the singlet of the methylene group into a doublet (indicated by the arrow) due to the loss of free rotation around CH_2-N and CH_2-Py bonds on formation of the metal chelate cycle.

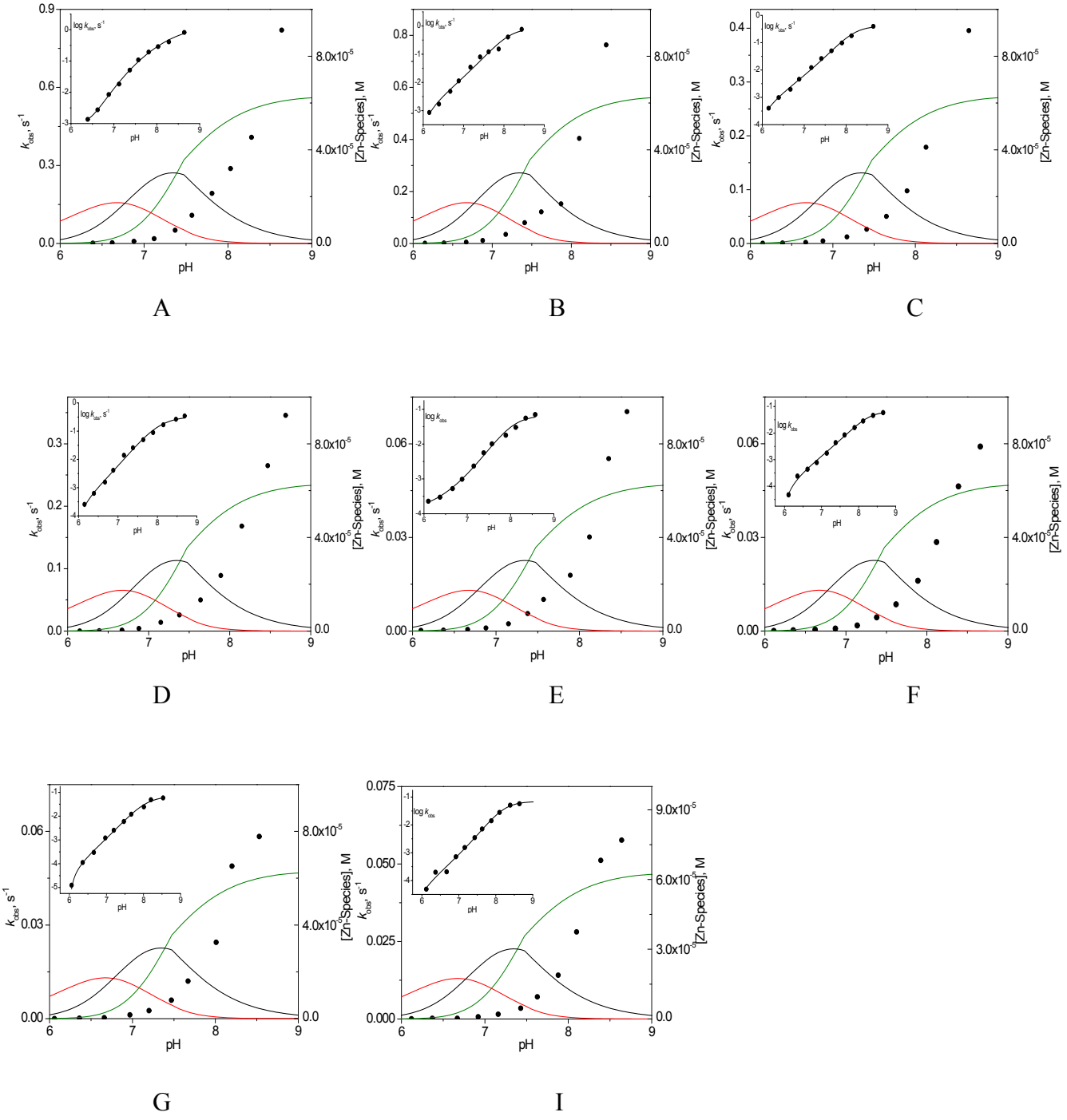

Fig. 7S. pH-rate profiles (solid circles) for the cleavage of 4-substituted phenyl acetates **5**a-**5**i in the presence of equimolar mixtures 0.1 mM of **L1** and zinc nitrate in water, 25°C, superimposed with the species distribution curves at the same conditions (right Y-axis). $[Zn(H\mathbf{L1})]^{2+}$ (red curve), oximate $[Zn(\mathbf{L1})]^{+}$ (black curve), and $[Zn(\mathbf{L1})(OH^{-})]$ (green curve). The inset shows the fitting to equation with two apparent pK_a values derived for two reactive species generated by consecutive deprotonations. Substituent groups: (A) NO_2, (B) COOH, (C) Ph, (D) Cl, (E) H, (F) Me, (G) i-Pr, (I) OMe

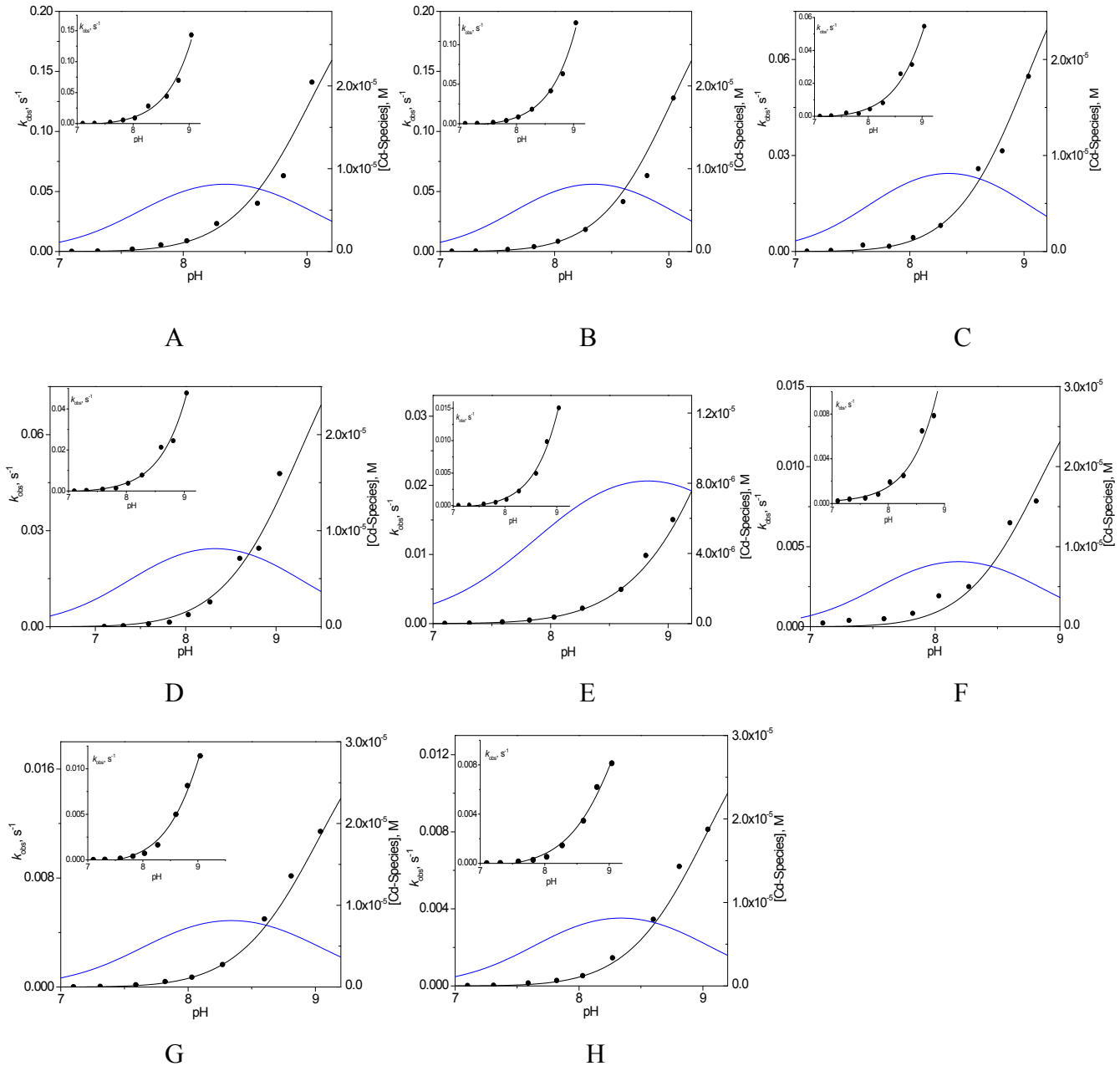

Fig. 8S. pH-rate profiles (solid circles) for the cleavage of 4-substituted phenyl acetates **5**a-**5**i in the presence of equimolar mixtures 0.1 mM of **L1** and cadmium nitrate in water, 25°C, superimposed with the species distribution curves at the same conditions (right Y-axis). $[Cd(H\mathbf{L1})]^{2+}$ (blue curve), $[Cd(\mathbf{L1})]^{+}$ (black curve). The inset shows the fitting to one apparent pK_a equation derived for one reactive specie generated by deprotonation. Substituent groups: (A) NO_2, (B) COOH, (C) Ph, (D) Cl, (E) H, (F) Me, (G) i-Pr, (H) OMe

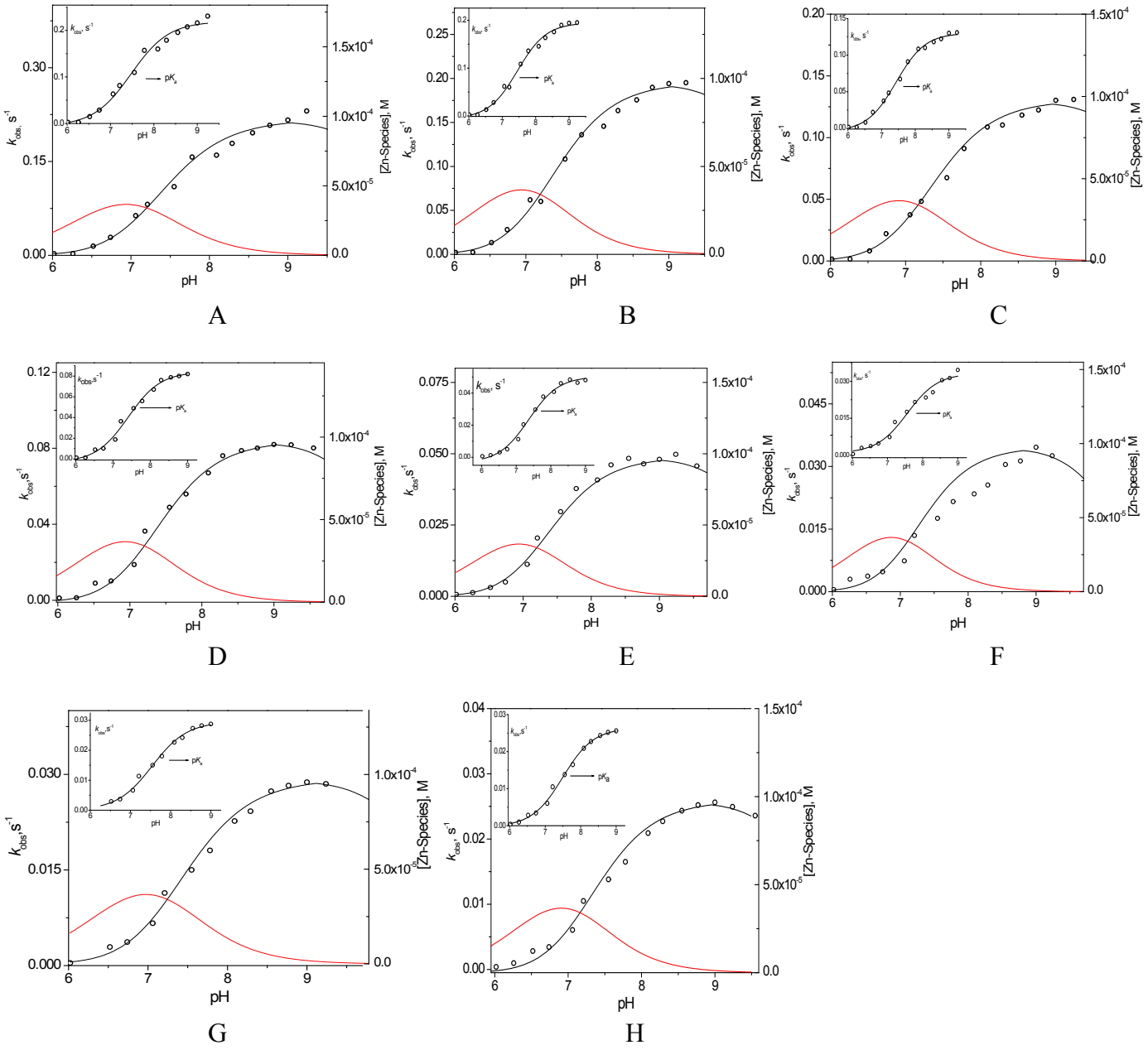

Fig. 9S. pH-rate profiles (open circles) for the cleavage of 4-substituted phenyl acetates **5**a-**5**i in the presence of equimolar mixtures 0.1 mM of **L2** and zinc nitrate in water, 25°C, superimposed with the species distribution curves at the same conditions (right Y-axis). $[Zn(H\mathbf{L2})]^{2+}$ (red curve), $[Zn(\mathbf{L2})]^{+}$ (black curve). The inset shows the fitting to one apparent pK_a equation derived for one reactive species generated by deprotonation. Substituent groups: (A) NO_2, (B) COOH, (C) Ph, (D) Cl, (E) H, (F) Me, (G) i-Pr, (H) OMe

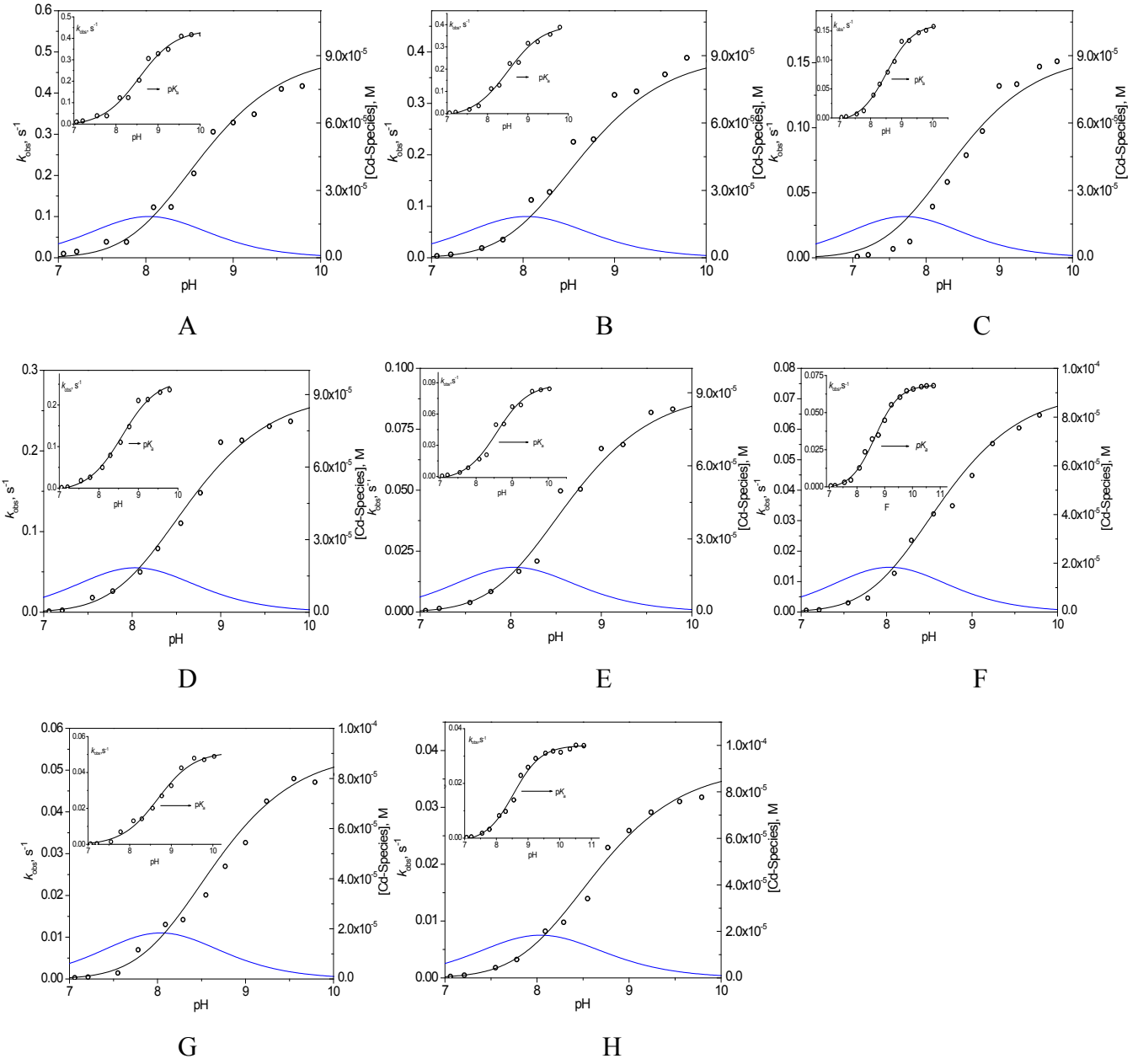

Fig. 10S. pH-rate profiles (open circles) for the cleavage of 4-substituted phenyl acetates **5**a-**5**i in the presence of equimolar mixtures 0.1 mM of **L2** and cadmium nitrate in water, 25°C, superimposed with the species distribution curves at the same conditions (right Y-axis). $[Cd(H\mathbf{L2})]^{2+}$ (blue curve), $[Cd(\mathbf{L2})]^{+}$ (black curve). The inset shows the fitting to one apparent pK_a equation derived for one reactive species generated by deprotonation. Substituent groups: (A) NO_2, (B) COOH, (C) Ph, (D) Cl, (E) H, (F) Me, (G) i-Pr, (H) OMe

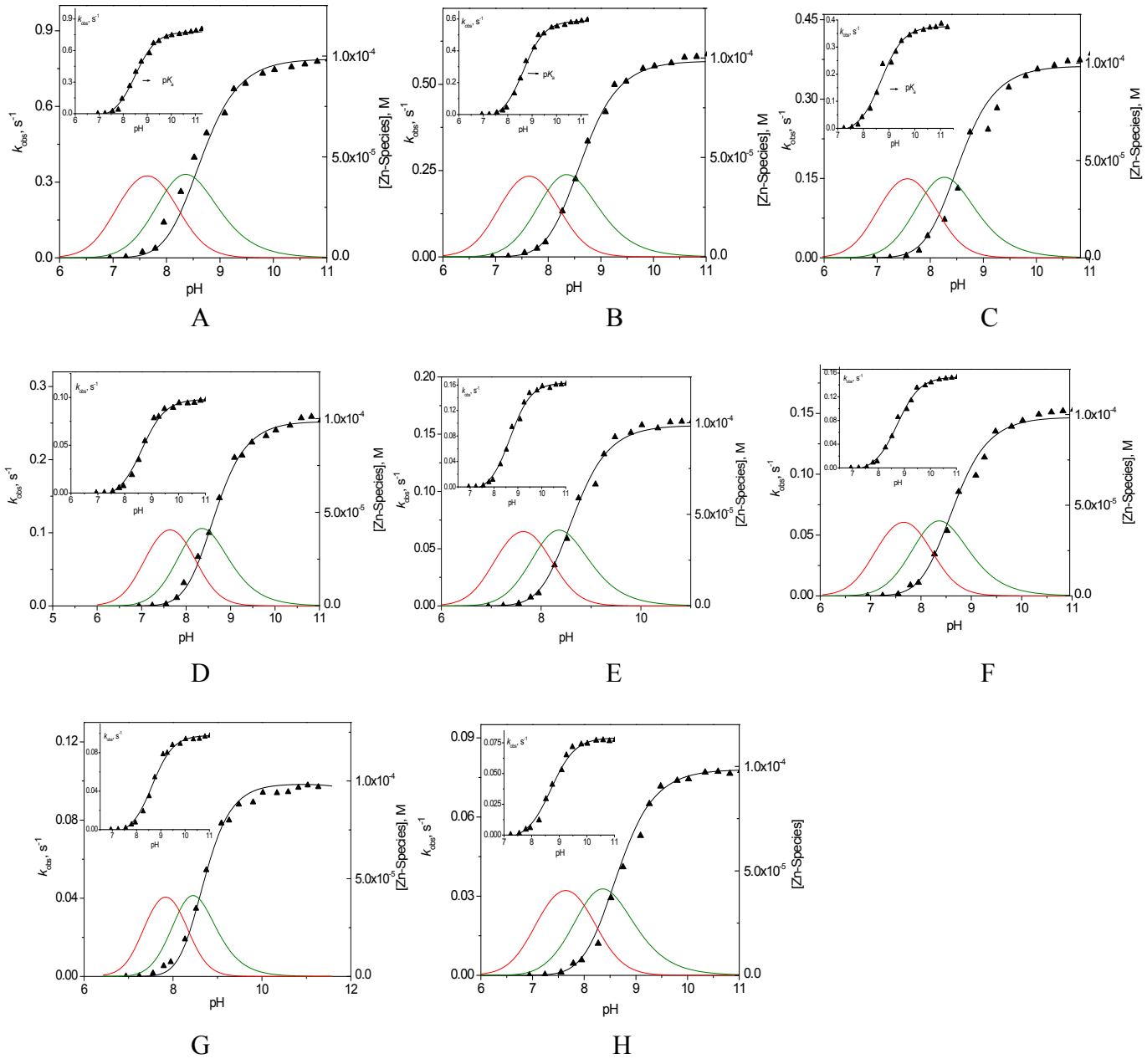

Fig. 11S. pH-rate profiles (solid triangles) for the cleavage of 4-substituted phenyl acetates **5**a-**5**i in the presence of equimolar mixtures 0.1 mM of **L3** and zinc nitrate in water, 25°C, superimposed with the species distribution curves at the same conditions (right Y-axis). $[Zn(H\mathbf{L3})]^{2+}$ (red curve), $[Zn(H\mathbf{L3})(OH)]^{+}$ (green curve), $[Zn(\mathbf{L3})(OH)]$ (black curve). The inset shows the fitting to one apparent pK_a equation derived for one reactive species generated by deprotonation. Substituent groups: (A) NO_2, (B) COOH, (C) Ph, (D) Cl, (E) H, (F) Me, (G) i-Pr, (H) OMe

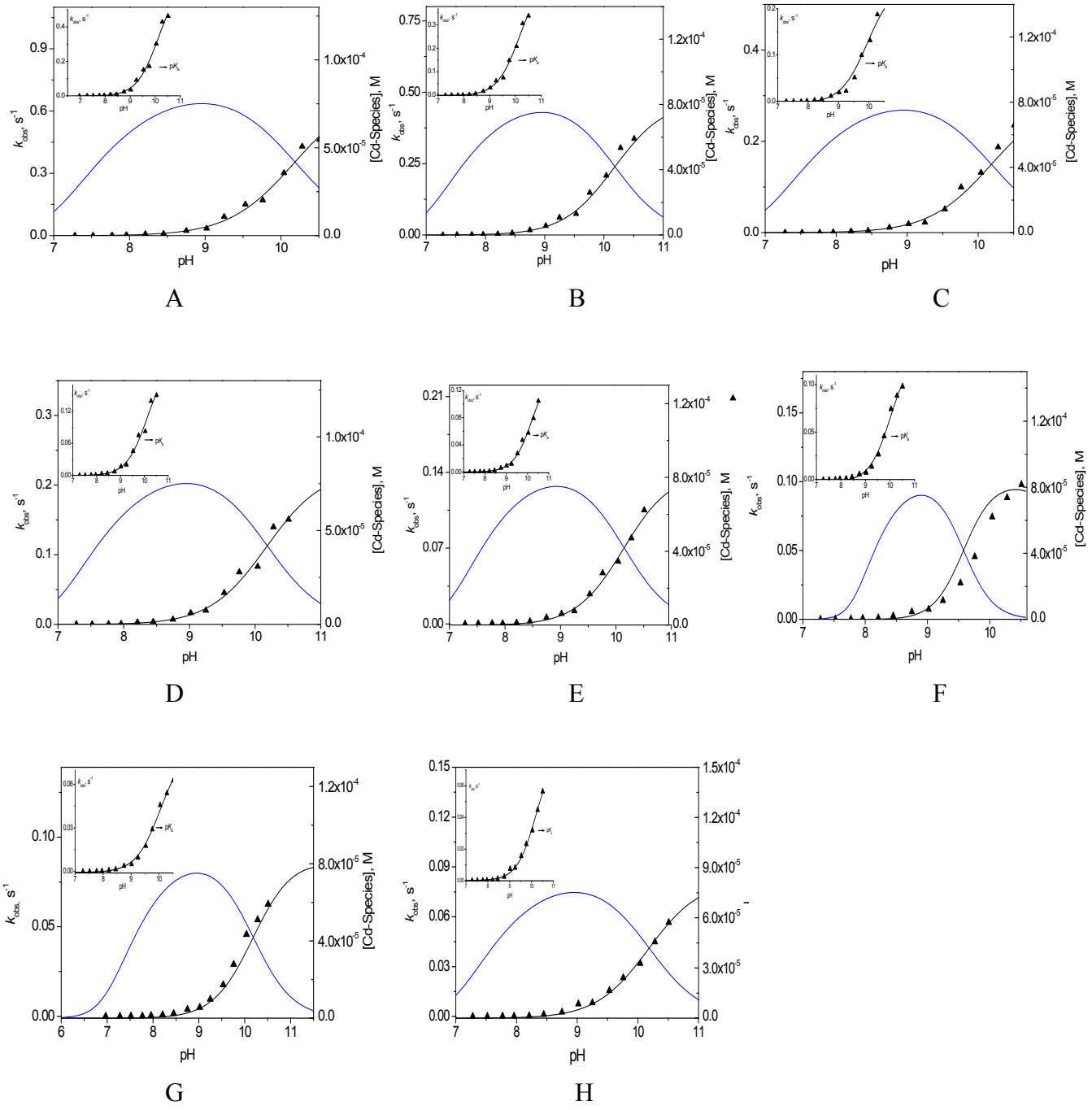

Fig. 12S. pH-rate profiles (open circles) for the cleavage of 4-substituted phenyl acetates **5**a-**5**i in the presence of equimolar mixtures 0.1 mM of **L3** and cadmium nitrate in water, 25°C, superimposed with the species distribution curves at the same conditions (right Y-axis). $[Cd(H\mathbf{L3})]^{2+}$ (blue curve), $[Cd(\mathbf{L3})]^{+}$ (black curve). The inset shows the fitting to one apparent pK_a equation derived for one reactive species generated by deprotonation. Substituent groups: (A) NO_2, (B) COOH, (C) Ph, (D) Cl, (E) H, (F) Me, (G) i-Pr, (H) OMe

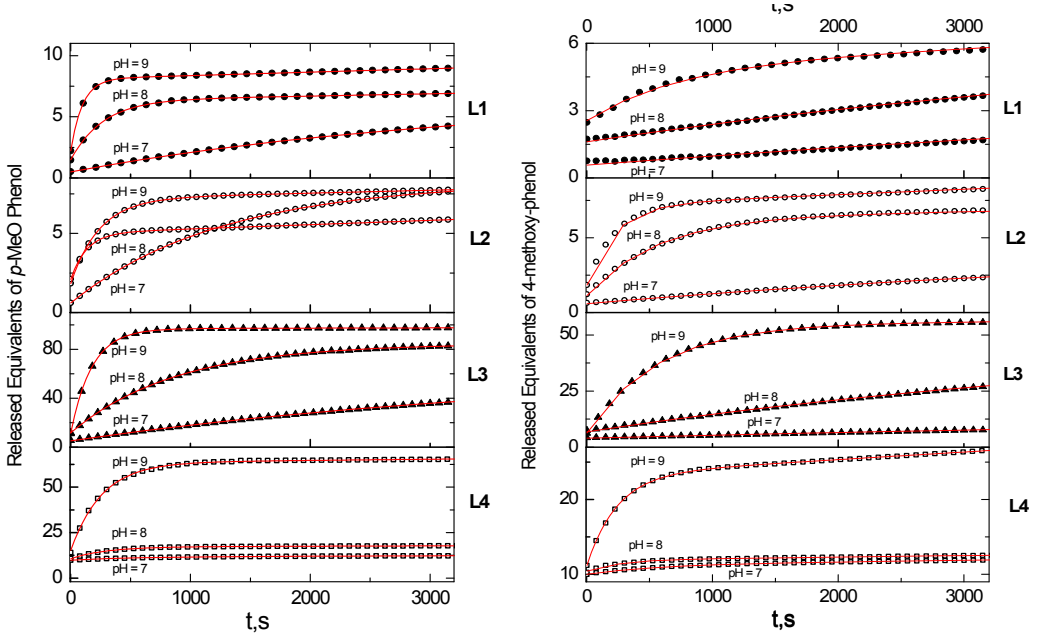

Zn(II) Cd(II)

Fig. 13S. Equivalents of 4-methoxy phenol released during the cleavage of **5**i 1mM in the presence of zinc and cadmium and ligands **L1- L4** at different pH values, 0.01 mM zinc or cadmium nitrate, 0.01 mM ligand in 0.1 M buffered aqueous solutions at 25°C. Continuous lines are the fitting to the first order reaction equation.

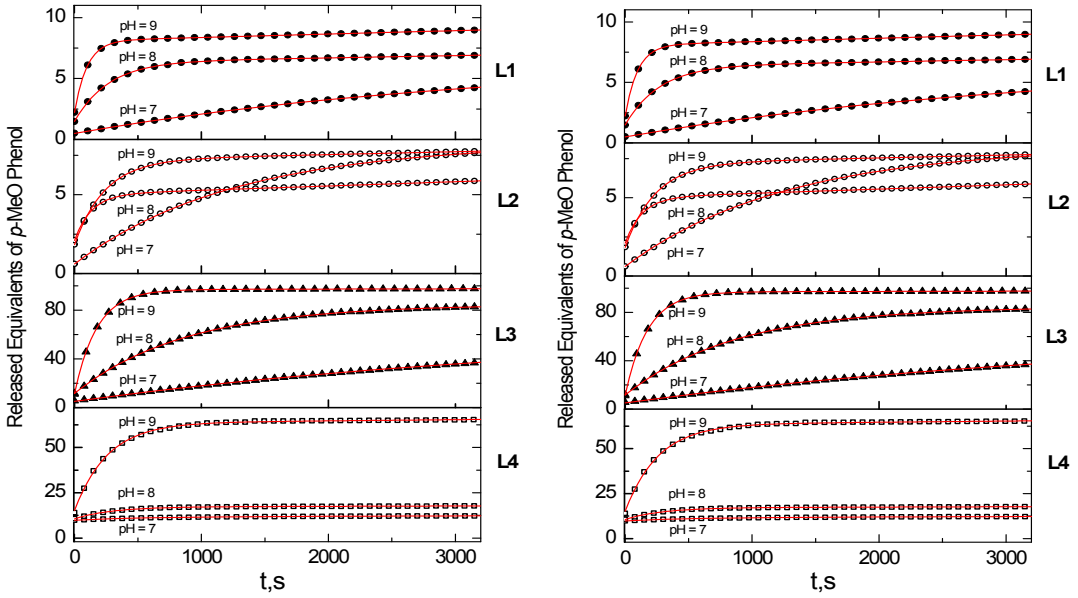

Zn(II) Cd(II)

Fig. 14S. Equivalents of 4-nitrophenol released during the cleavage of **5**a 1mM in the presence of zinc and cadmium and ligands **L1- L4** at different pH values, 0.01 mM zinc or cadmium nitrate, 0.01 mM ligand in 50 mM buffered aqueous solutions at 25°C. Continuous lines are the fitting to the first order reaction equation.

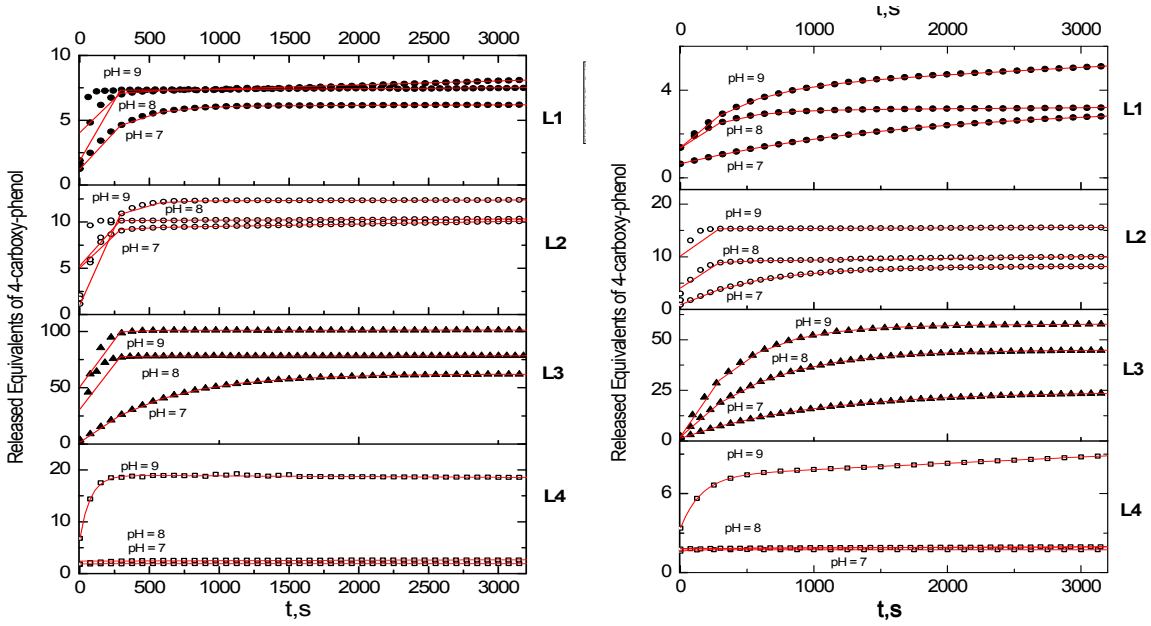

Zn(II) Cd(II)

Fig. 15S. Equivalents of 4-carboxyphenol released during the cleavage of **5**b 1 mM in the presence of zinc and cadmium and ligands **L1**- **L4** at different pH values, 0.01 mM zinc or cadmium nitrate, 0.01 mM ligand in 50 mM buffered aqueous solutions at 25°C. Continuous lines are the fitting to the first order reaction equation.

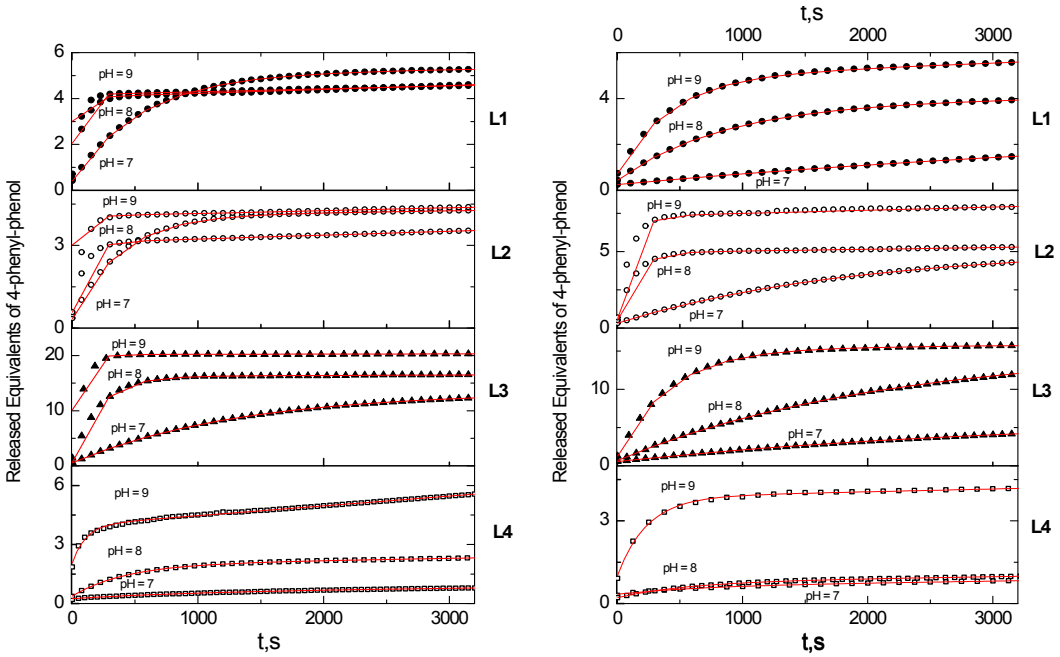

Zn(II) Cd(II)

Fig. 16S. Equivalents of 4-phenylphenol released during the cleavage of **5**c 1 mM in the presence of zinc and cadmium and ligands **L1**- **L4** at different pH values, 0.01 mM zinc or cadmium nitrate, 0.01 mM ligand in 50 mM buffered aqueous solutions at 25°C. Continuous lines are the fitting to the first order reaction equation.

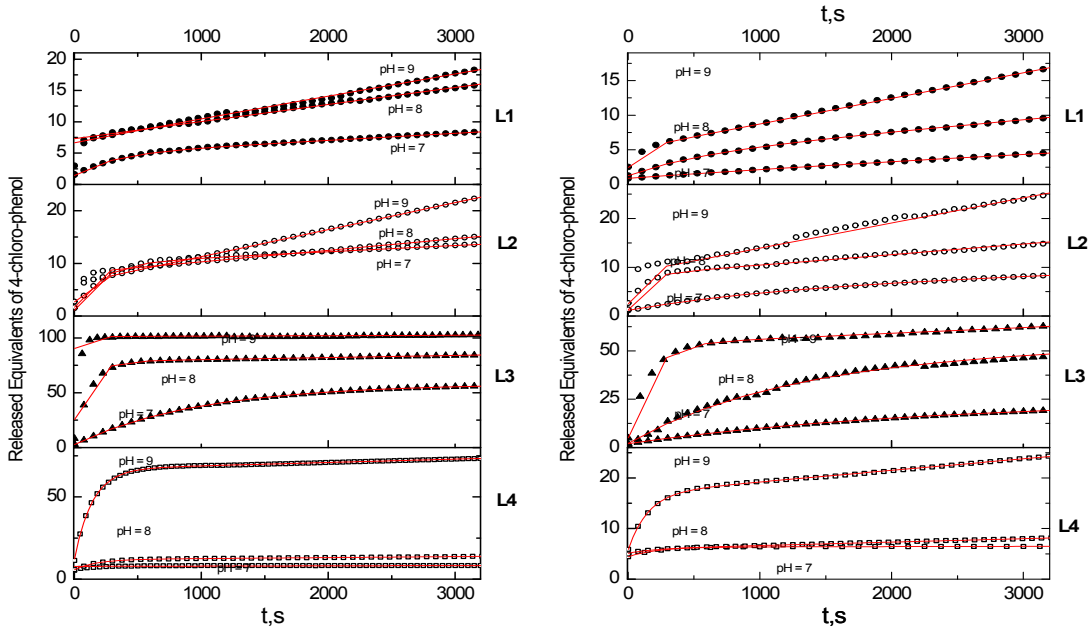

Zn(II) Cd(II)

Fig. 17S. Equivalents of 4-chlorophenol released during the cleavage of **5**d 1 mM in the presence of zinc and cadmium and ligands **L1- L4** at different pH values, 0.01 mM zinc or cadmium nitrate, 0.01 mM ligand in 50 mM buffered aqueous solutions at 25°C. Continuous lines are the fitting to the first order reaction equation.

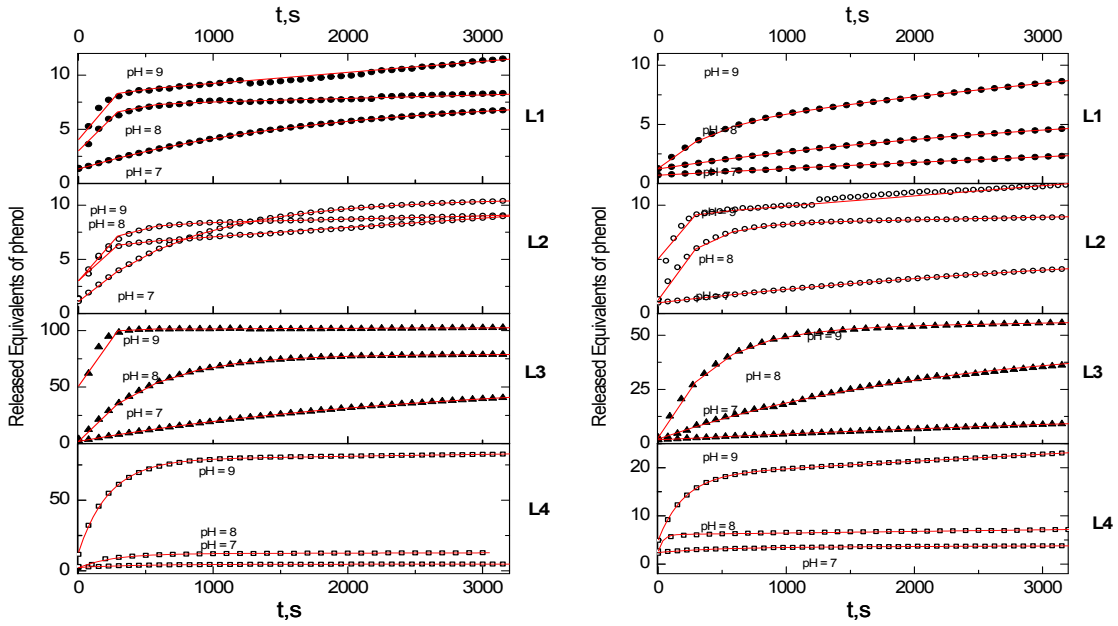

Zn(II) Cd(II)

Fig. 18S. Equivalents of phenol released during the cleavage **5**e 1mM in the presence of zinc and cadmium and ligands **L1- L4** at different pH values, 0.01 mM zinc or cadmium nitrate, 0.01 mM ligand in 50 mM buffered aqueous solutions at 25°C. Continuous lines are the fitting to the first order reaction equation.

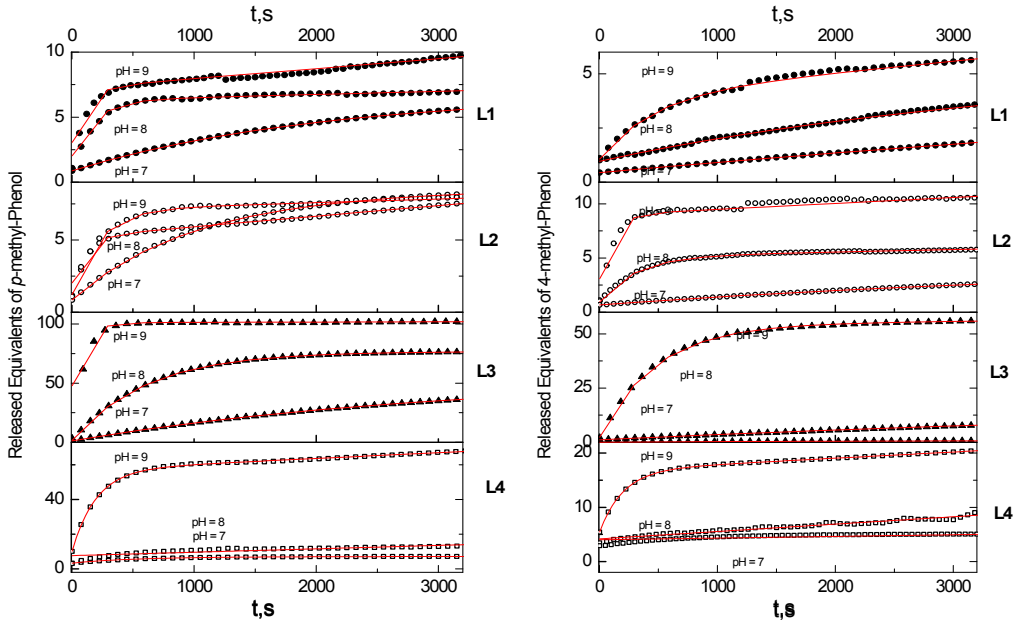

Fig. 19S. Equivalents of 4-methyl phenol released during the cleavage of **5**f 1mM in the presence of zinc and cadmium and ligands **L1- L4** at different pH values, 0.01 mM zinc or cadmium nitrate, 0.01 mM ligand in 50 mM buffered aqueous solutions at 25°C. Continuous lines are the fitting to the first order reaction equation.

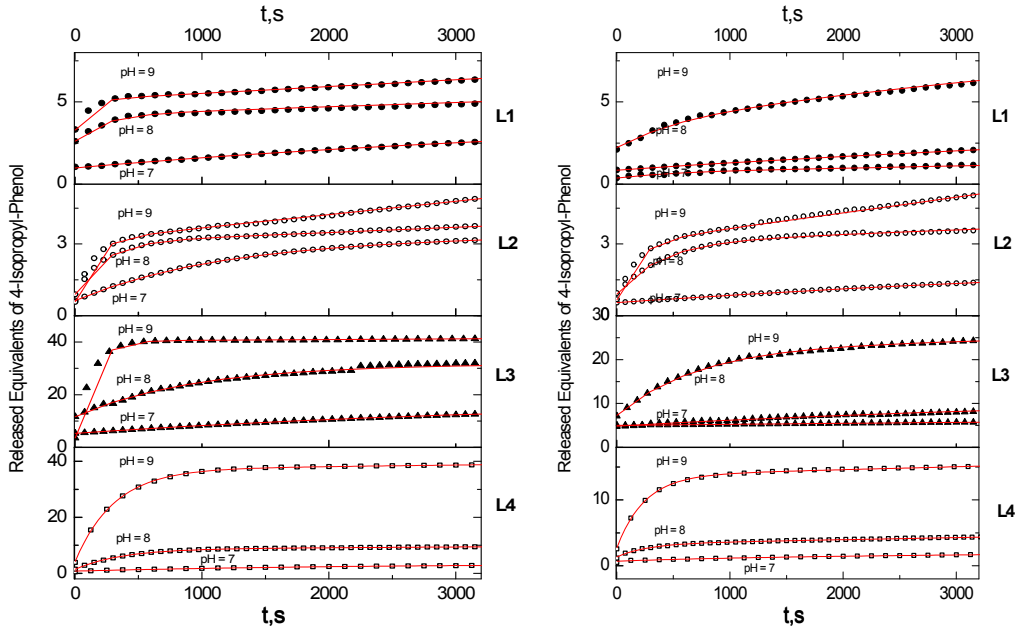

Fig. 20S. Equivalents of 4-isopropylphenol released during the cleavage of **5**g 0.40 mM in the presence of zinc and cadmium and ligands **L1- L4** at different pH values, 0.01 mM zinc or cadmium nitrate, 0.01 mM ligand in 50 mM buffered aqueous solutions at 25°C. Continuous lines are the fitting to the first order reaction equation.

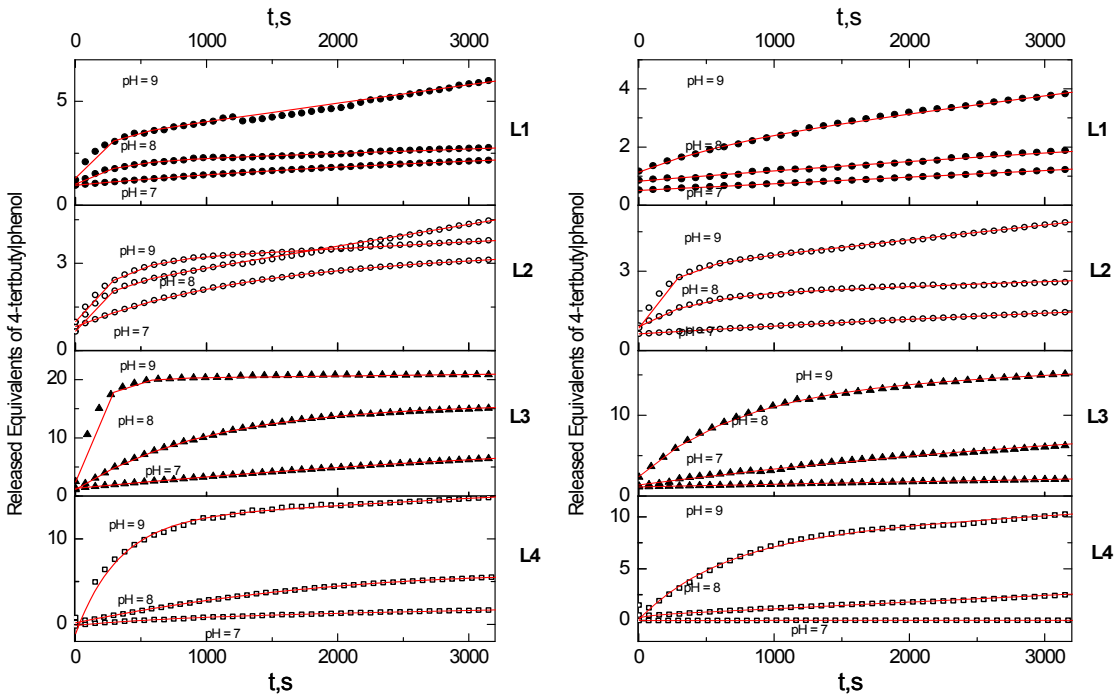

Fig. 21S. Equivalents of 4-tertbutylphenol released during the cleavage of **5**h 0.2 mM in the presence of zinc and cadmium and ligands **L1**- **L4** at different pH values, 0.01 mM zinc or cadmium nitrate, 0.01 mM ligand in 0.1 M buffered aqueous solutions at 25°C. Continuous lines are the fitting to the first order reaction equation.

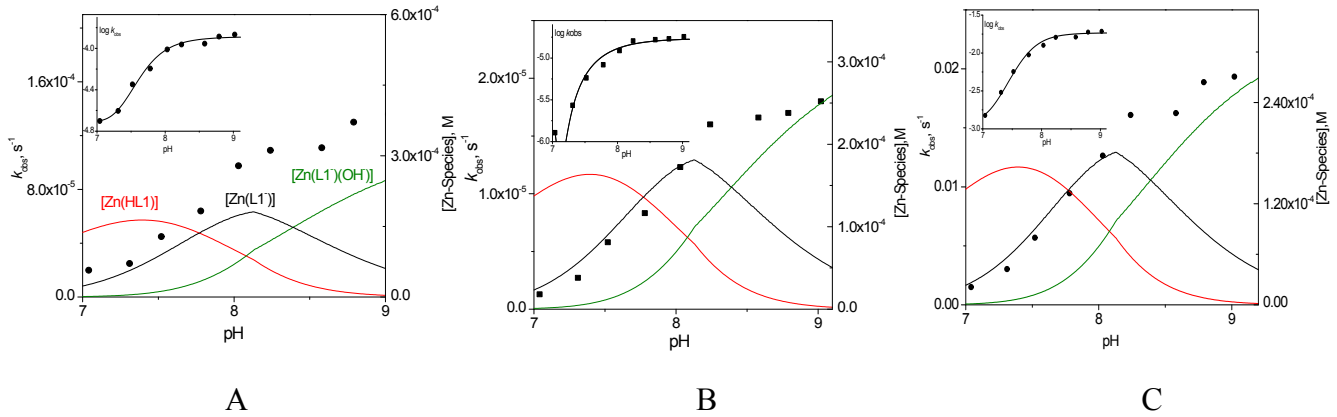

Fig. 22S. pH-rate profiles (solid circles) for the cleavage of **6** (A), **7** (B), and **8** (C) in the presence of equimolar mixtures 0.5 mM of **L1** and zinc perchlorate in water, 25°C, superimposed with the species distribution curves at the same conditions (right Y-axis). $[Zn(H\mathbf{L1})]^{2+}$ (red curve), oximate $[Zn(\mathbf{L1})]^{+}$ (black curve), and $[Zn(\mathbf{L1})(OH^{-})]$ (green curve). The inset shows the fitting to equation with two apparent pK_a values derived for two reactive species generated by consecutive deprotonations.

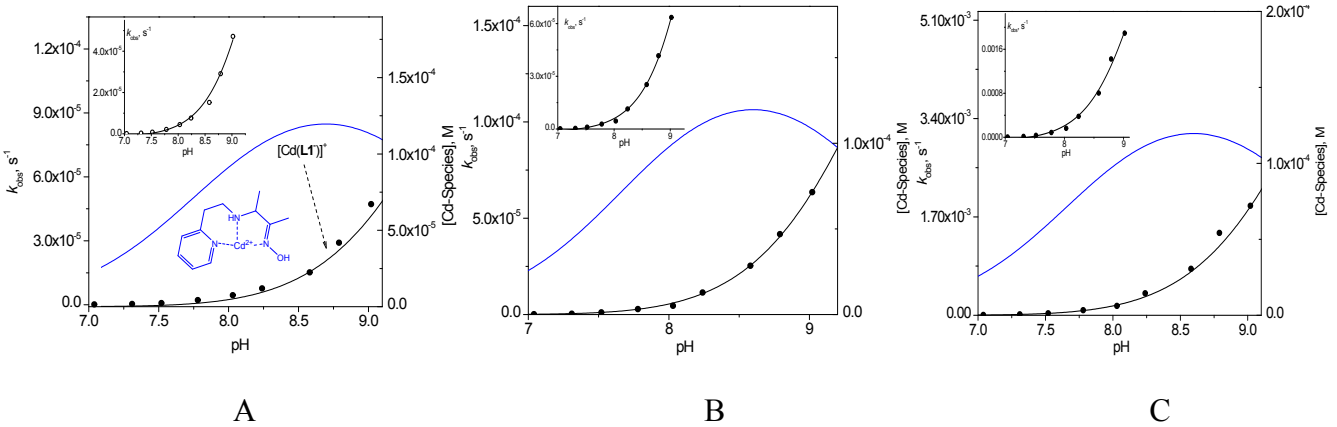

Fig. 23S. pH-rate profiles (solid circles) for the cleavage of **6** (A), **7** (B), and **8** (C) in the presence of equimolar mixtures 0.5 mM of **L1** and cadmium nitrate in water, 25°C, superimposed with the species distribution curves at the same conditions (right Y-axis). $[Cd(H\mathbf{L1})]^{2+}$ (blue curve), oximate $[Cd(\mathbf{L1})]^{+}$ (black curve). The inset shows the fitting to one apparent pK_a equation derived for one reactive specie generated by consecutive deprotonations.

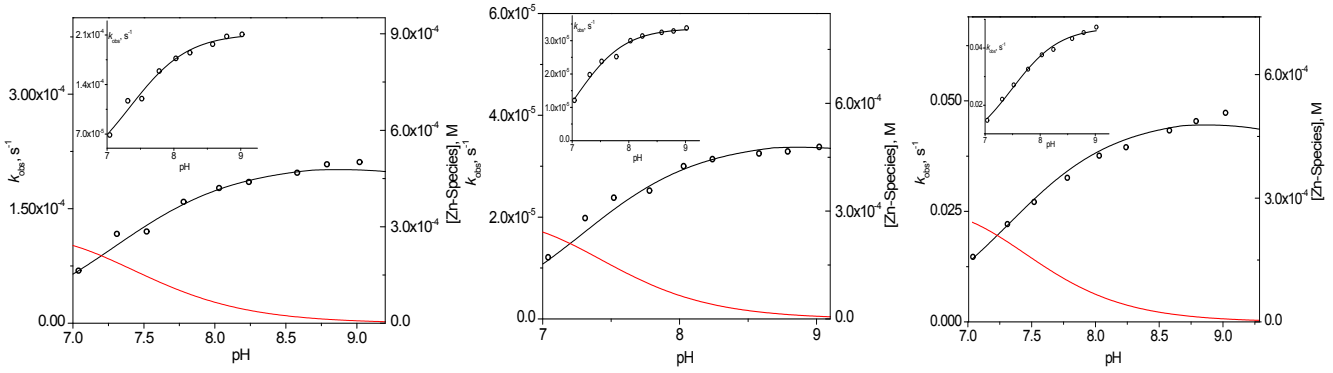

Fig. 24S. pH-rate profiles (open circles) for the cleavage of **6** (A), **7** (B), and **8** (C) in the presence of equimolar mixtures 0.5 mM of **L2** and zinc perchlorate in water, 25°C, superimposed with the species distribution curves at the same conditions (right Y-axis). $[Zn(H\mathbf{L2})]^{2+}$ (red curve), oximate $[Zn(\mathbf{L2})]^{+}$ (black curve). The inset shows the fitting to one apparent pK_a equation derived for one reactive specie generated by deprotonation.

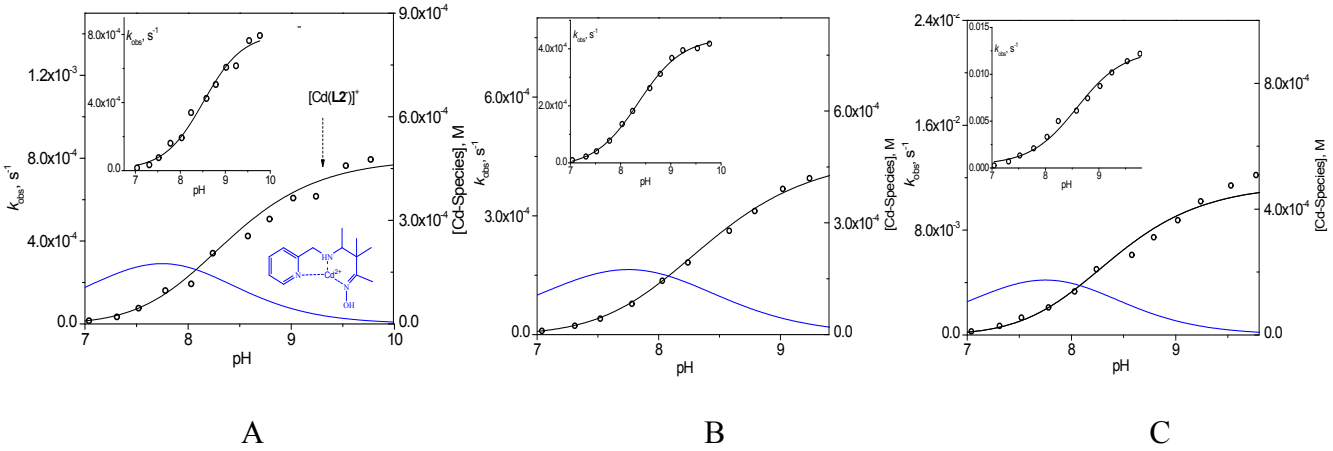

Fig. 25S. pH-rate profiles (open circles) for the cleavage of **6** (A), **7** (B), and **8** (C) in the presence of equimolar mixtures 0.5 mM of **L1** and cadmium nitrate in water, 25°C, superimposed with the species distribution curves at the same conditions (right Y-axis). $[Cd(H\mathbf{L2})]^{2+}$ (blue curve), oximate $[Cd(\mathbf{L2})]^{+}$ (black curve). The inset shows the fitting to one apparent pK_a equation derived for one reactive specie generated by deprotonation.

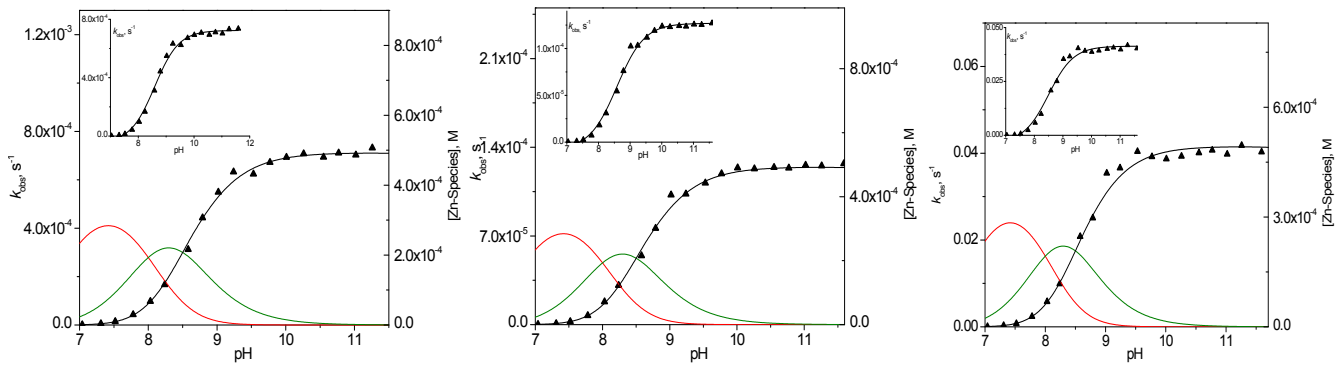

Fig. 26S. pH-rate profiles (solid triangles) for the cleavage of **6** (A), **7** (B), and **8** (C) in the presence of equimolar mixtures 0.5 mM of **L3** and zinc perchlorate in water, 25°C, superimposed with the species distribution curves at the same conditions (right Y-axis). $[Zn(H\mathbf{L3})]^{2+}$ (red curve), $[Zn(H\mathbf{L3})(OH)]^{+}$ (green curve), $[Zn(\mathbf{L3})(OH)]$ (black curve).. The inset shows the fitting to one apparent pK_a equation derived for one reactive specie generated by deprotonation.

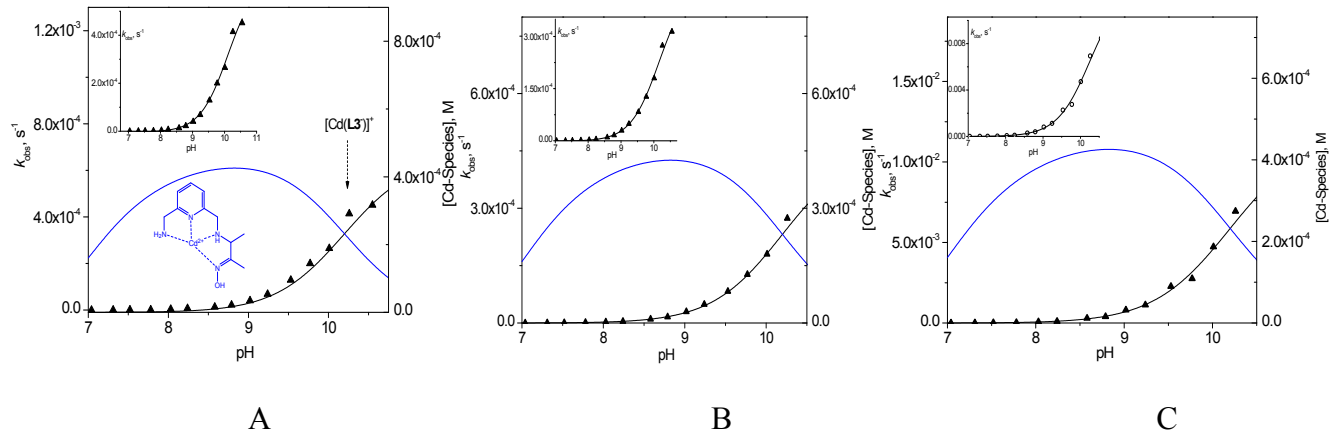

Fig. 27S. pH-rate profiles (solid triangles) for the cleavage of **6** (A), **7** (B), and **8** (C) in the presence of equimolar mixtures 0.5 mM of **L1** and cadmium nitrate in water, 25°C, superimposed with the species distribution curves at the same conditions (right Y-axis). $[Cd(H\mathbf{L3})]^{2+}$ (blue curve), oximate $[Cd(\mathbf{L3})]^{+}$ (black curve). The inset shows the fitting to one apparent pK_a equation derived for one reactive specie generated by deprotonation.

2-(pyridin-2-yl) ethanamine. To an aqueous solution of solid 2-(bromomethyl) pyridine hydrobromide (3.00 g, 11.86 mmol) solid dry $NaHCO_3$ was added (1.00 g, 11.86 mmol,1 equiv). The neutral compound was extracted with ethyl ether (3 × 30 mL), the organic layer was dried with anhydrous $MgSO_4$ and the solvent was removed under reduced pressure. The resulting solid (2.50 g, 9.88 mmol) was mixed in ethanol (30 mL) with NaCN (0.48 g, 9.88 mmol) and this mixture was refluxed for 24 h at 75 °C, the solvent volume was reduced and a white solid, 2-(cyanomethyl) pyridine, was obtained by cooling down the mixture to -5 °C. A solution of sodium borohydride (0.26 g, 7.00 mmol) in 30 mL of ethyl ether was added dropwise to a mixture of 2-(cyanomethyl) pyridine (0.80 g, 6.82 mmol) and $AlCl_3$ (0.93 g, 7.00 mmol). The solution was stirred at room temperature until the disappearance of the reactant followed by TLC, approximately 6 h. The solvent was removed and the resulting mixture was extracted with hot isopropyl ether (3 × 30 mL). Organic layers were combined and the solvent was removed under reduced pressure to yield 0.60 g (40%) of 2-(2-aminoethyl) pyridine as a pale yellow oil. ^{1}H NMR (400 MHz, $CDCl_3$) δ 8.55 (ddd, *J* = 4.9, 1.6, 0.8 Hz, 1H), 7.61 (td, *J* = 7.7, 1.9 Hz, 1H), 7.20 – 7.11 (m, 1H), 3.12 (t, *J* = 6.7 Hz, 1H), 2.94 (t, *J* = 6.7 Hz, 1H), 1.51 (s, 1H).

3-((2-(pyridin-2-yl)ethyl)amino)butan-2-one oxime (L1). To a 2 mL of solution of 2-(pyridin-2-yl)ethanamine (500 mg, 4.09 mmol) in isopropyl ether was added 1 mL of 2,3-butanodione monoxime (410 mg, 4.09 mmol) in the same solvent. The reaction mixture was refluxed at 65°C during 4h to yield 85% of the imine as a white pure solid (0.72 g, 3.48 mmol). Reduction of the imine (500 mg, 2.4 mmol) was carried out in 20 mL of dry methanol by adding dropwise a cooled methanolic solution of $NaBH_4$ (73 mg, 1.93 mmol, 0.8 equiv) with continuous stirring at 5 °C. The reaction mixture was stirred at room temperature for another 2 h; the solvent was removed under reduced pressure, 10 mL of distilled water was added, and pH was adjusted to 10.30. The final product was extracted in CH_2Cl_2 (3×50 mL), dried over anhydrous $MgSO_4$ and the removal of the solvent yielded 28% of ligand **2** as a pale yellow solid (0.69 g, 3.33 mmol). ^{1}H NMR (400 MHz, DMSO-d6) δ 10.31 (s, 1H), 8.45 (ddd, *J* = 4.8, 0.9 Hz, 1H), 7.66 (td, *J* = 7.6, 1.9 Hz, 1H), 7.24 – 7.15 (m, 2H), 3.25 (q, *J* = 6.7 Hz, 1H), 2.89 – 2.64 (m, 4H), 1.61 (s, 2H), 1.05 (d, *J* = 6.7 Hz, 3H). ^{13}C NMR (101 MHz, DMSO-d6) δ 160.7, 158.7, 149.3, 136.7, 123.5, 121.6, 56.9, 47.5, 38.4, 19.5, 8.7. MS (APCI, m/z) 208.1402 [MH+; calcd for $C_{11}H_{18}N_3O$: 208.1449]. Anal. Calcd for $C_{11}H_{17}N_3O$: C, 63.74; H, 8.27; N, 20.27. Found: C, 63.22 ± 0.23; H, 7.69 ± 0.66; N, 19.68 ± 0.46. IR (FTIR-ATR, ν_{max} in cm^{-1}): 3253 (s), 3154 (m), 3048 (m), 3008 (s), 2971 (s), 2905 (s), 2841 (s), 2722 (s), 1728 (w), 1652 (w), 1590 (s), 1568 (m), 1473 (s), 1442 (s), 1367 (m), 1328 (w), 1265 (w), 1202 (w), 1154 (w), 1138 (m), 1108 (s), 1072 (m), 1044 (m), 992

(s), 948 (s), 886 (s), 825 (m), 784 (m), 769 (m), 750 (m), 646 (w), 632 (w), 609 (w), 579 (w), 525 (w), 447 (w), 404 (w).

2,4-pentanedione,3,3-dimethyl-,2-oxime. A solution of 3,3-dimethylpentane-2,4-dione (1 g, 7.8 mmol) in methanol (5 mL) was prepared and stirred at room temperature. A suspension of hydroxylammonium chloride (0.54 g, 7.8 mmol, 1 equiv) in methanol (5 mL) was neutralized by adding NaOH (1 equiv., in 2 mL of water) an then it was added dropwise to the former solution during 20 min. The mixture was left under stirring at room temperature overnight and then the solvent was removed under reduced pressure. An aqueous slurry was obtained to which 20 mL of hexane at 5 °C were added to afford a white solid (0.65 g, 5.8 mmol) which is the mono substituted oxime (yield of 58%). ^{1}H NMR (300 MHz, $CDCl_3$) δ 2.82 (s, 1H), 1.93 (s, 3H), 1.52 (s, 3H), 1.16 (s, 3H), 1.03 (s, 3H).

3,3-dimethyl-4-((pyridin-2-ylmethyl)amino)pentan-2-one oxime (L2).

The synthesis of **L2** under harsh condensation conditions with one-pot reductive amination was preferred over the Schiff-base isolation. Solid 2,4-pentanedione, 3,3-dimethyl-,2-oxime (0.5 g, 3.49 mmol) was dissolved in a minimum volume of chloroform (3 mL) and then a suspension of sodium triacetoxy borohydride (0.74 g, 3.49 mmol, 1 equiv) in 15 mL of acetic acid was added dropwise under stirring. The mixture was left 24 h under stirring at room temperature and the excess of solvent was removed under reduced pressure. The residue was mixed with tetramethyl ammonium hydroxide pentahydrate (TMAOH) in a 10 mL of 50:50 v/v methanol-water at pH 10. The solvent was removed under reduced pressure and then 20 mL of chloroform were added. The formed solid was separated by filtration and discarded as an inorganic salt. Then the chloroform solution was slowly evaporated and after that a solid began to precipitate and it was isolated by filtration to afford 0.098 g of **L2** (12%). ^{1}H NMR (301 MHz, DMSO-d_6) δ 10.44 (s, 1H), 8.54 – 8.43 (m, 1H), 7.72 (td, *J* = 7.7, 1.8 Hz, 1H), 7.45 – 7.14 (m, 2H), 3.64 (q, *J* = 5.0 Hz, 2H), 3.28 (q, *J* = 6.7 Hz, 1H), 1.71 (s, 3H), 1.13 (d, *J* = 8.1 Hz, 3H), 1.07 (s, 6H). ^{13}C NMR (101 MHz, DMSO-d6) δ 160.3, 158.1, 148.7, 136.5, 121.9, 120.2, 59.2, 56.2, 52.1, 34.1, 19.2, 8.5. MS (APCI, m/z) 236.1749 [MH+; calcd for $C_{13}H_{22}N_3O$: 236.1763]. Anal. Calcd for $C_{13}H_{21}N_3O$: C, 66.35; H, 8.99; N, 17.86. Found: C, 65.91 ± 0.17; H, 8.35 ± 0.33; N, 17.33 ± 0.21. IR (FTIR-ATR, ν_{max} in cm^{-1}): 3261 (s), 3031 (m), 2710 (w), 2699 (w), 2664 (m), 2632 (s), 2571 (s), 2466 (s), 1400 (s), 1382 (w), 1261 (s), 1238 (s), 1473 (s), 1175 (m), 1158 (m), 1067 (w), 888 (s), 830 (m), 648 (m), 609 (s), 536 (m).

2,6-bis(aminomethyl) pyridine. According with the literature methodology,[2] a Delépine reaction was carried out starting from solid 2,6-bis(bromomethyl) pyridine (5.00 g, 18.87 mmol), it was mixed with solid hexamethylenetetramine (10.0 g, 71.33 mmol) and refluxed in 60 mL of CH_2Cl_2 during 6 h. The white solid formed was filtered off, dried under vacuum and then dissolved in 40 mL of an acidic ethanol solution (HCl 10 % v/v). This mixture was refluxed at 70°C during 18 h and the solid hydrochloride the 2,6-bis(aminomethyl) pyridine was filtered off, washed with hot methanol (5×20 mL) and dried. ^{1}H NMR (300 MHz, DMSO-d6) δ 7.68 (t, *J* = 7.7 Hz, 1H), 7.25 (d, *J* = 7.7 Hz, 2H), 3.75 (s, 4H), 1.93 (br, 4H).

3-(((6-(aminomethyl)pyridin-2-yl)methyl)amino)butan-2-one oxime (L3). To a solution of the hydrochloride of 2,6-bis(aminomethyl) pyridine (1.00 g, 4.06 mmol) in a solvent mixture of diisopropyl ether (60%), CH_2Cl_2 (30 %) and CH_3OH (10%), 3 equivalents of tetramethylammonium hydroxide (2.20 g, 12.18 mmol) were added, followed by the addition of 2,3-butanodione monoxime (410 mg, 4.06 mmol) in small amounts during 1 h. The solvent was then removed under vacuum and a solid product was obtained. This solid was washed with hot dioxane (5 × 15 mL) to obtain the organic products, a mixture of the mono (80 %) and disubstituted (20%) imine. The desired monosubstituted imine was successfully separated from the solid by washing it with CH_2Cl_2 and isolated as a yellow oil after removing the CH_2Cl_2. The monosubstituted imine (500 mg, 2.27 mmol) was dissolved in 20 mL of dry methanol and a cooled methanolic solution of $NaBH_4$ (73 mg, 1.93 mmol) was added dropwise while stirring at 5 °C. The reaction mixture was allowed to reach room temperature, stirred for 2 h and the solvent was then removed under reduced pressure. The residue was dissolved in 10 mL of deionized water, the pH was adjusted to 10.70 and the solution was extracted with CH_2Cl_2 (3 × 50 mL) and dried over anhydrous $MgSO_4$, yielding 23% of **L3** (0.95 g, 4.27 mmol) as a pale yellow oil after solvent removal. ^{1}H NMR (400 MHz, $CDCl_3$) δ 10.88 (s, 1H), 7.57 (t, *J* = 7.6 Hz, 1H), 7.35 – 6.98 (m, 2H), 3.95 (s, 2H), 3.79 (s, 2H), 3.43 (q, *J* = 6.7, 13.4 Hz, 1H), 1.84 (s, 3H), 1.24 (d, *J* = 6.7 Hz, 3H). ^{13}C NMR (101 MHz, $CDCl_3$) δ 160.4, 159.5, 159.0, 137.2, 120.8, 119.7, 56.9, 52.4, 47.1, 19.3, 9.1. MS (APCI, m/z) 223.1433 [MH+; calcd for $C_{11}H_{19}N_4O$: 223.1559]. Anal. Calcd for $C_{11}H_{18}N_4O$: C, 59.44; H, 8.16; N, 25.20. Found: C, 58.83 ± 0.17; H, 8.13 ± 0.48; N, 24.71 ± 0.17. IR (FTIR-ATR, ν_{max} in cm^{-1}): 3187 (s), 3066 (s), 2920 (s), 2852 (s), 1660 (w), 1593 (m), 1576 (m), 1453 (s), 1366 (m), 1323 (w), 1221 (w), 1117 (w), 1030 (w), 975 (m), 937 (m), 774(m), 624 (w), 564 (w), 445 (w).

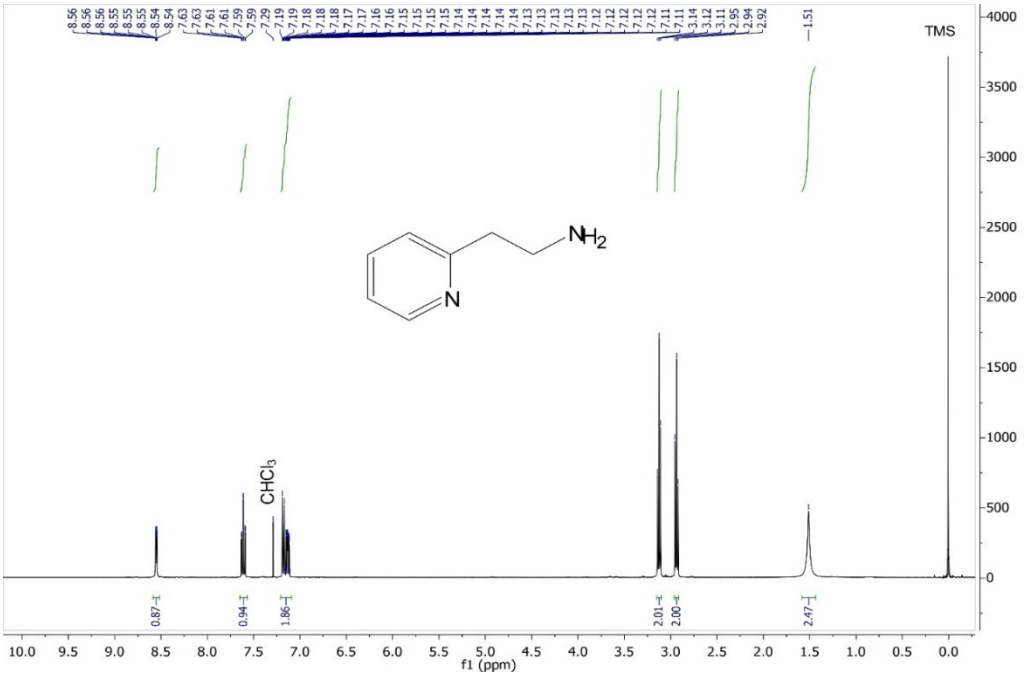

Fig 28S. ^{1}H-NMR spectra of 2-(pyridin-2-yl) ethanamine in DMSO-$_{d6}$

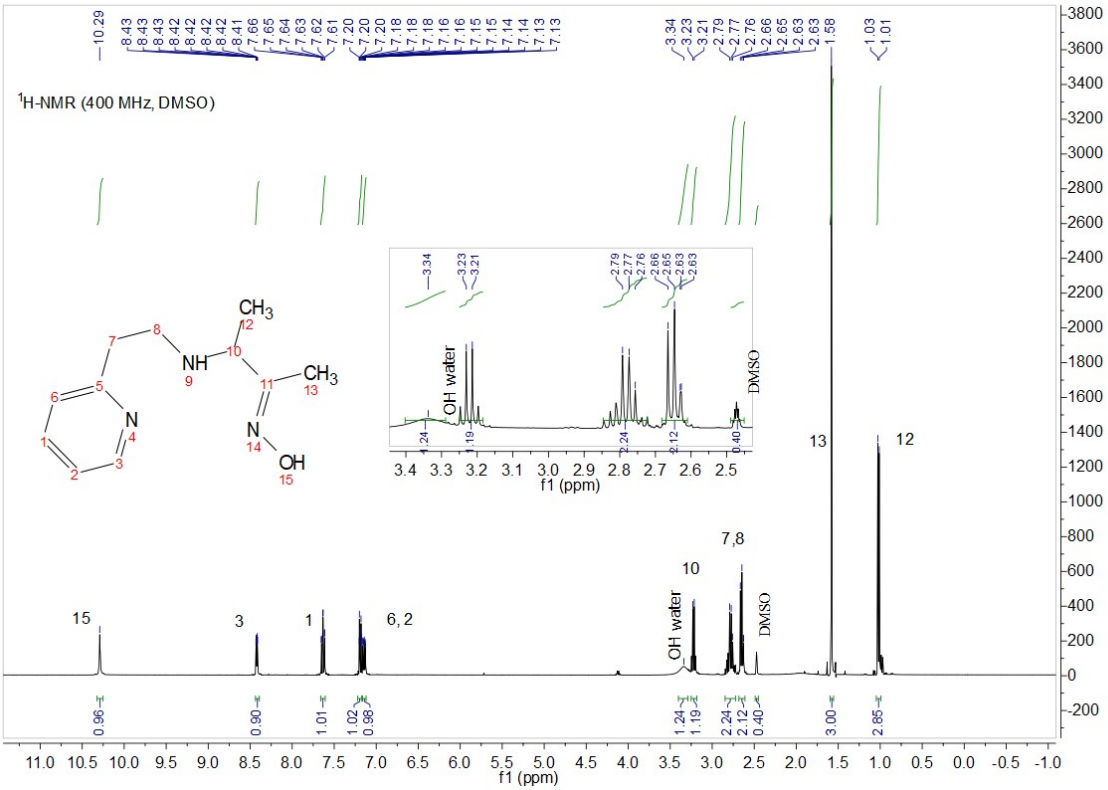

Fig 29S. ^{1}H-NMR spectra of **L1** in DMSO-$_{d6}$

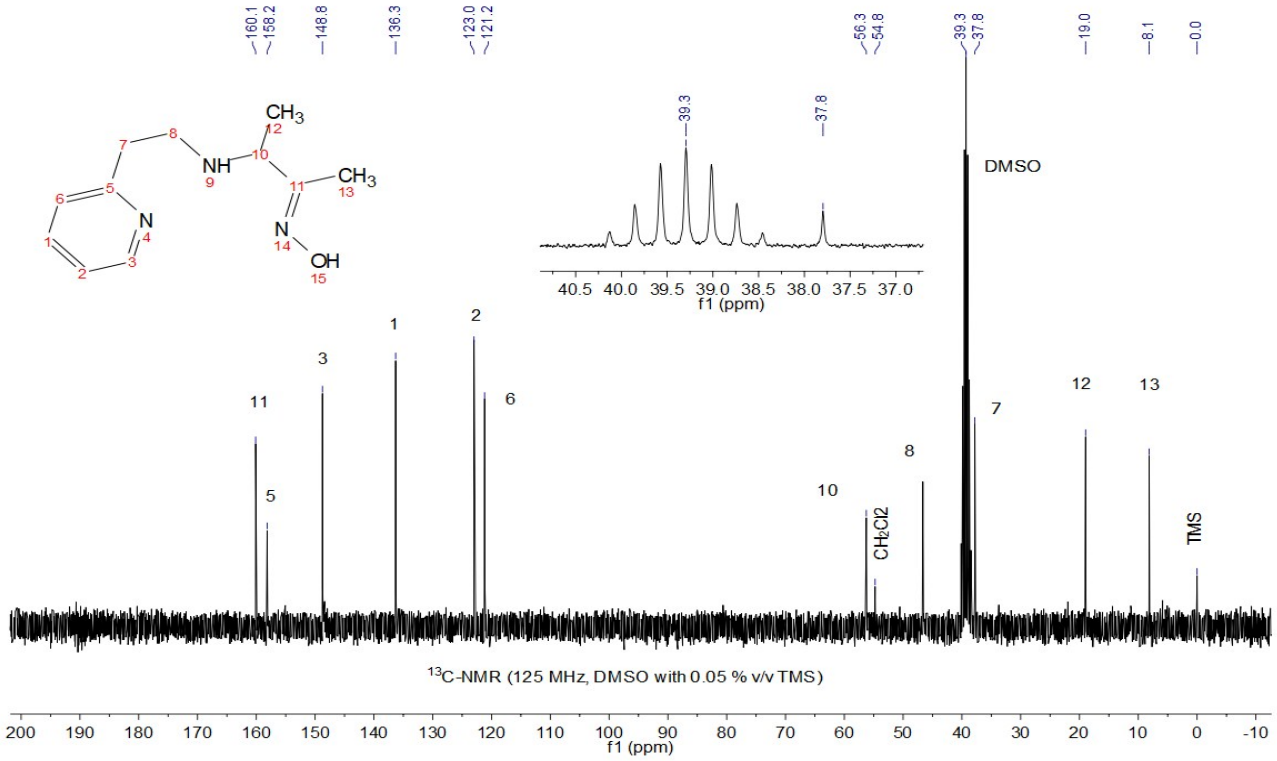

Fig 30S. ^{13}C-NMR spectra of **L1** in DMSO-$_{d6}$

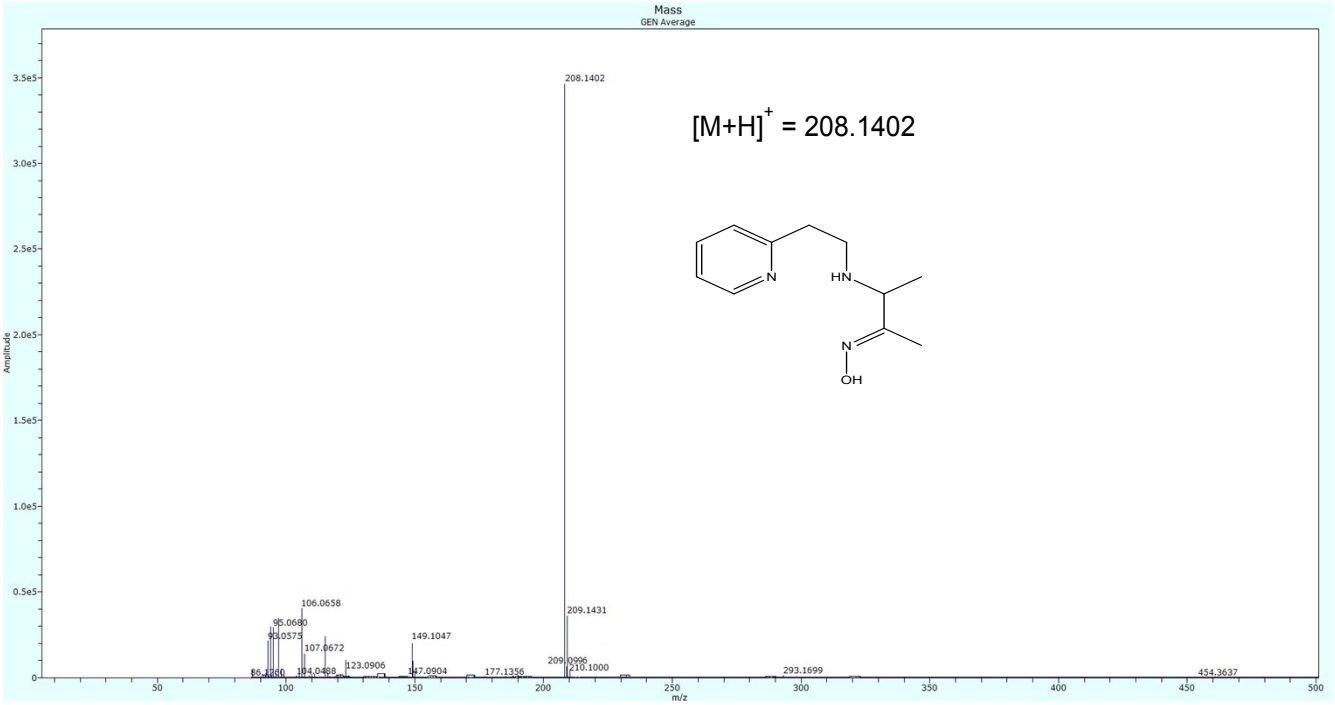

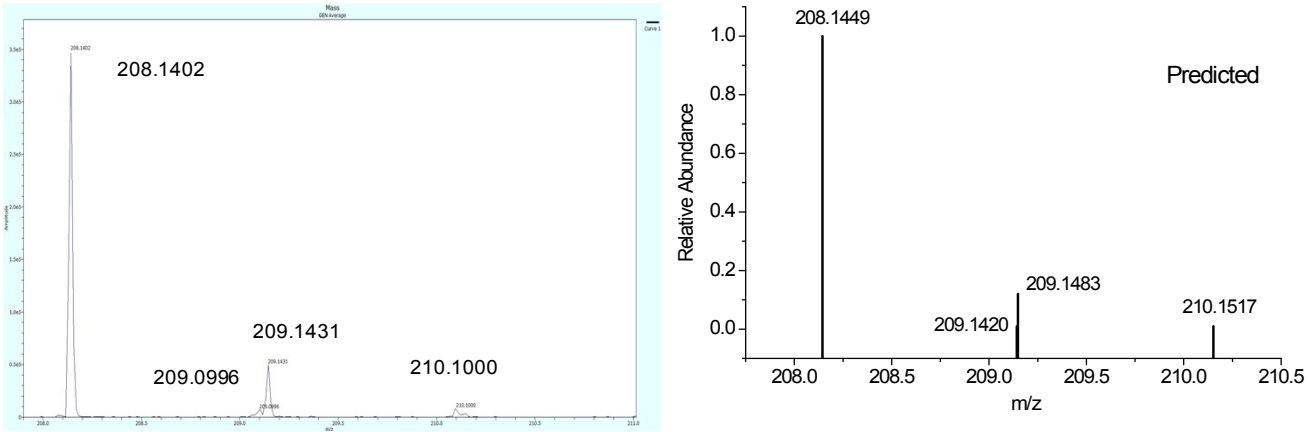

Fig 31S. APCI-mass spectrum (positive mode) of **L1.** High resolution $[M+H]^+$ 208.1402 and comparison of experimental *vs.* calculated m/z values.

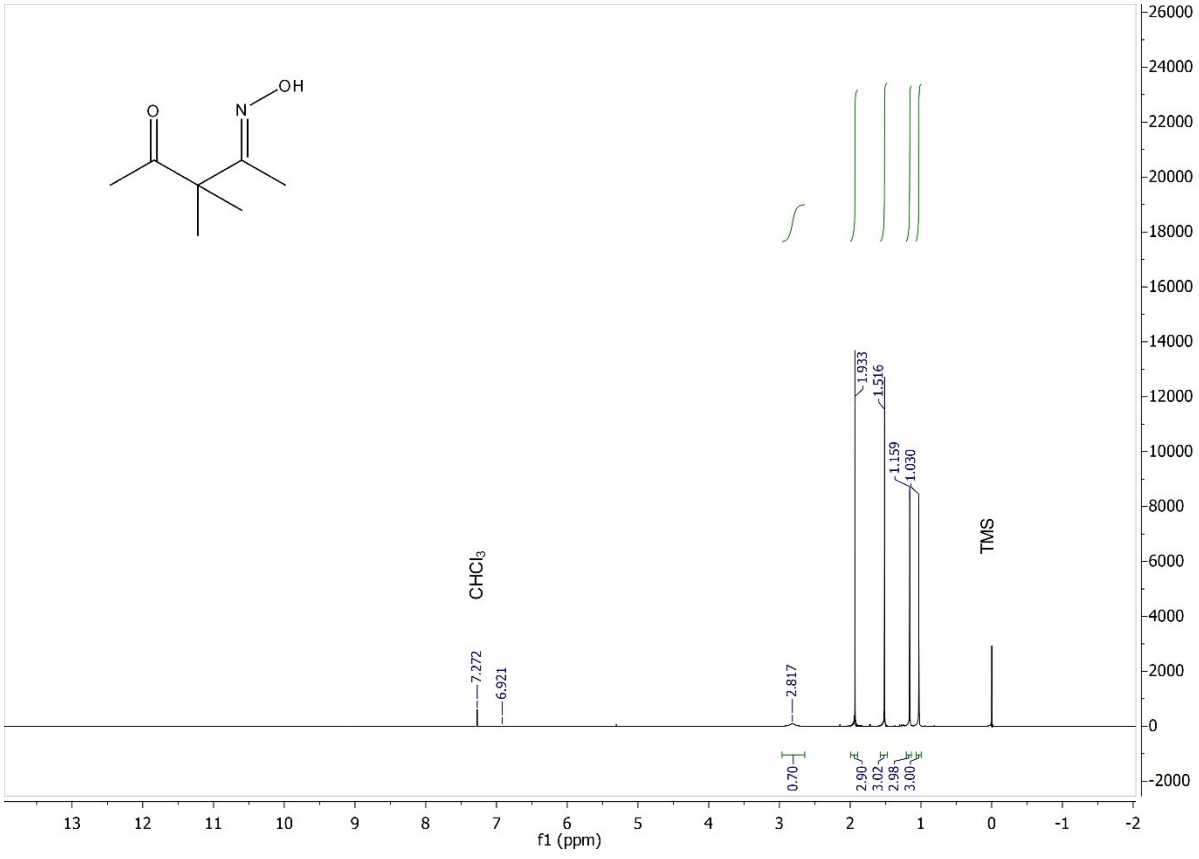

Fig 32S. ^{1}H-NMR spectra of 2,4-pentanedione,3,3-dimethyl-,2-oxime in DMSO-$_{d6}$

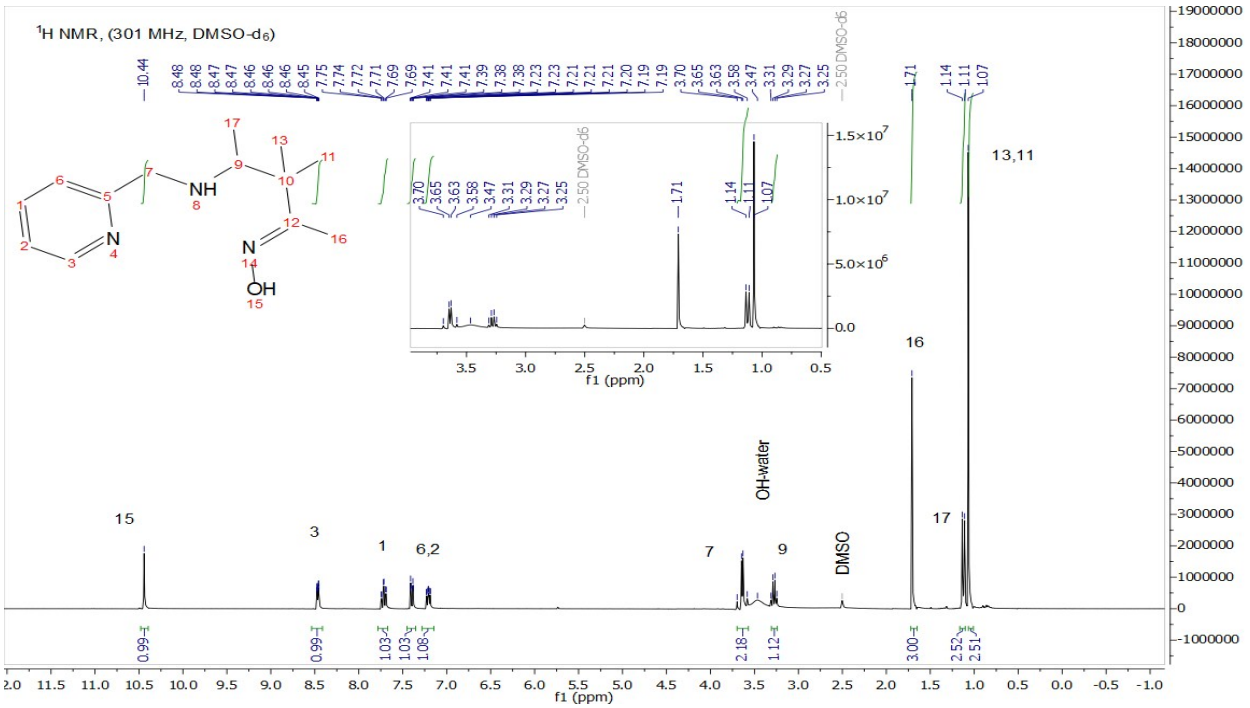

Fig 33S. ^{1}H-NMR spectra of **L2** in DMSO-$_{d6}$

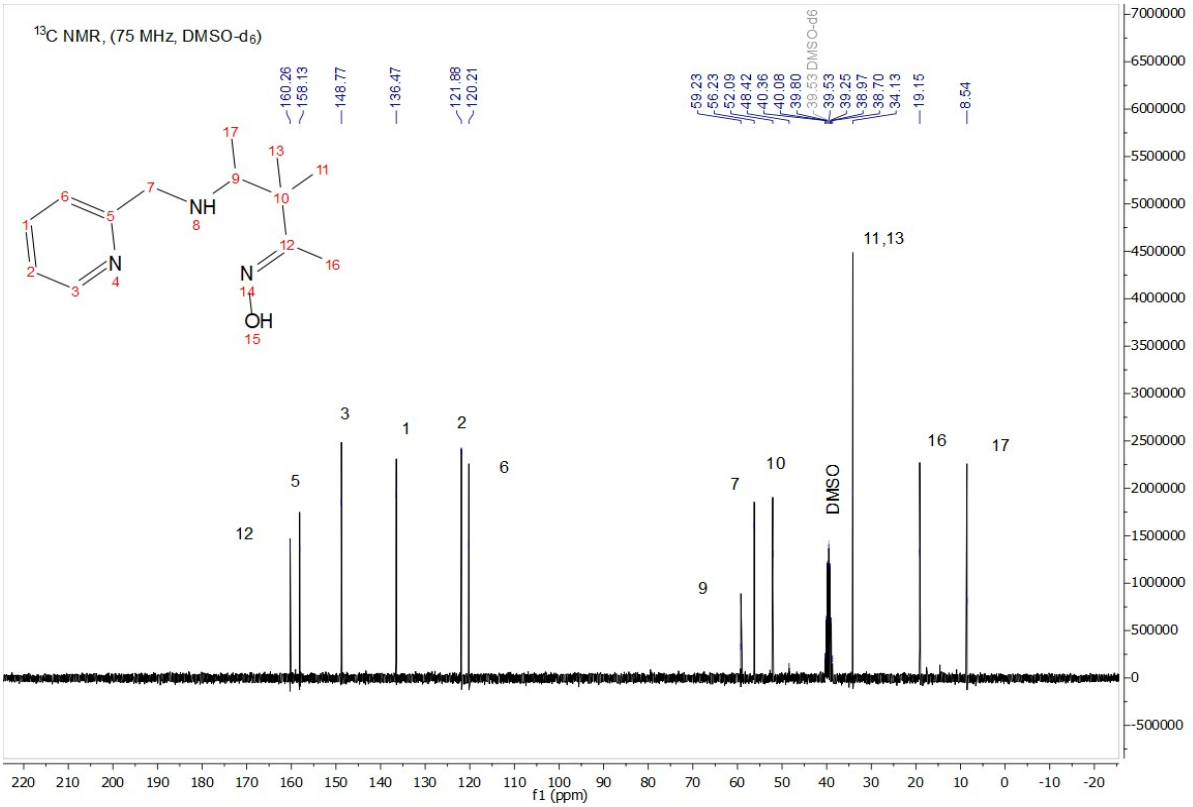

Fig 34S. ^{13}C-NMR spectra of **L2** in DMSO-d_6

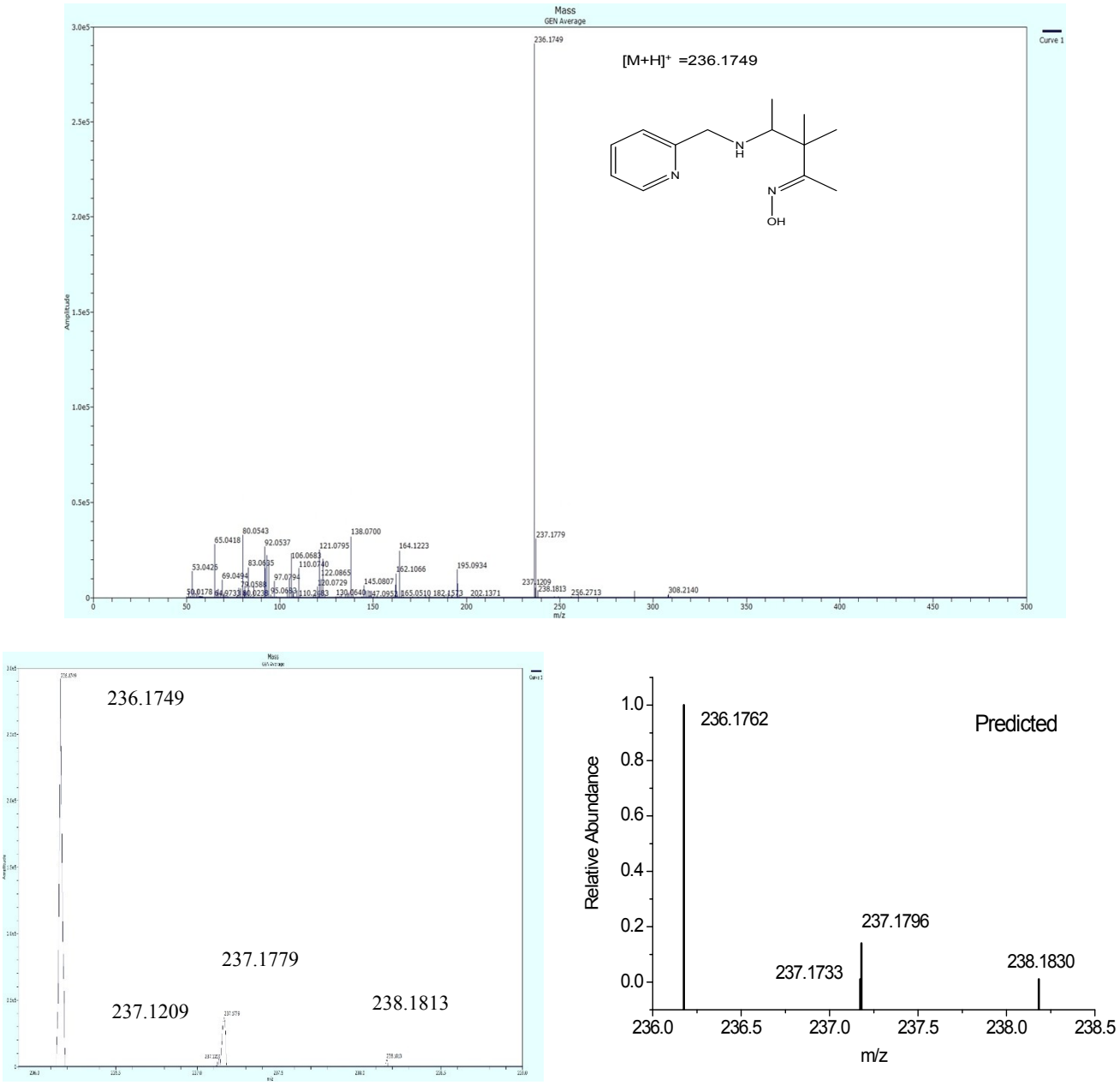

Fig 35S. APCI-mass spectrum (positive mode) of **L2.** High resolution $[M+H]^+$ 236.1749 and comparison of experimental *vs.* calculated values.

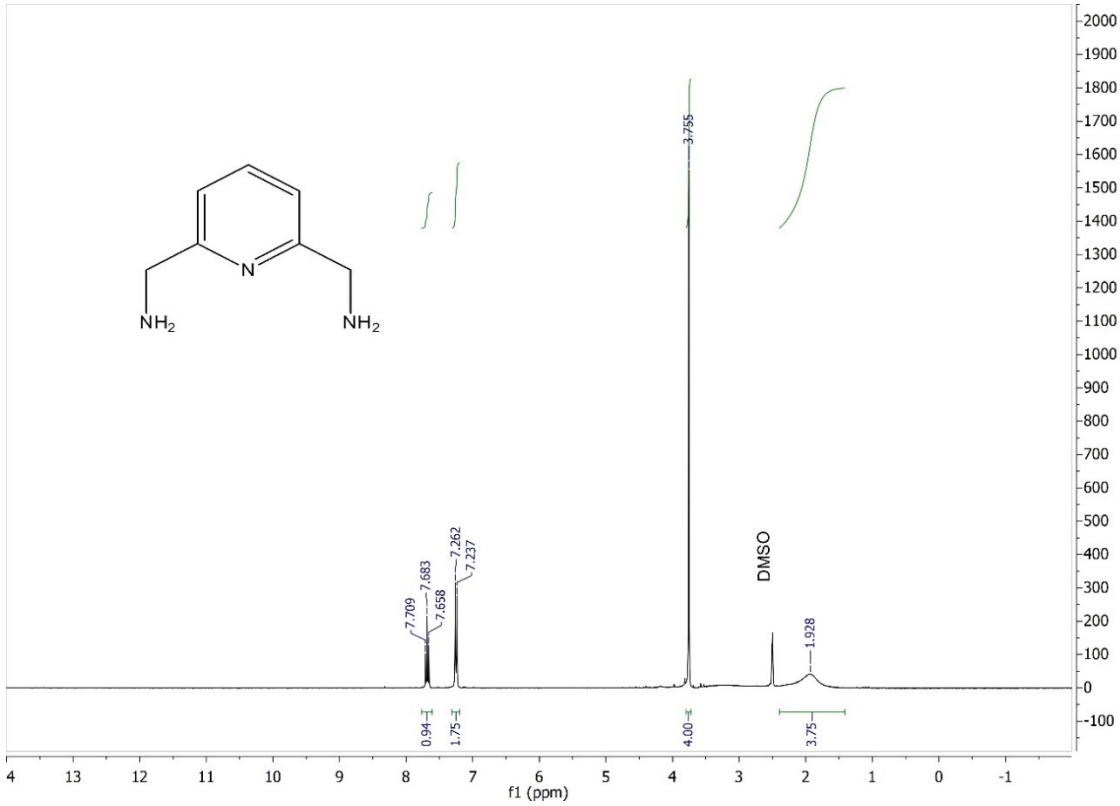

Fig 36S. ^{1}H-NMR spectra of 2,6-bis(aminomethyl) pyridine in DMSO-$_{d6}$

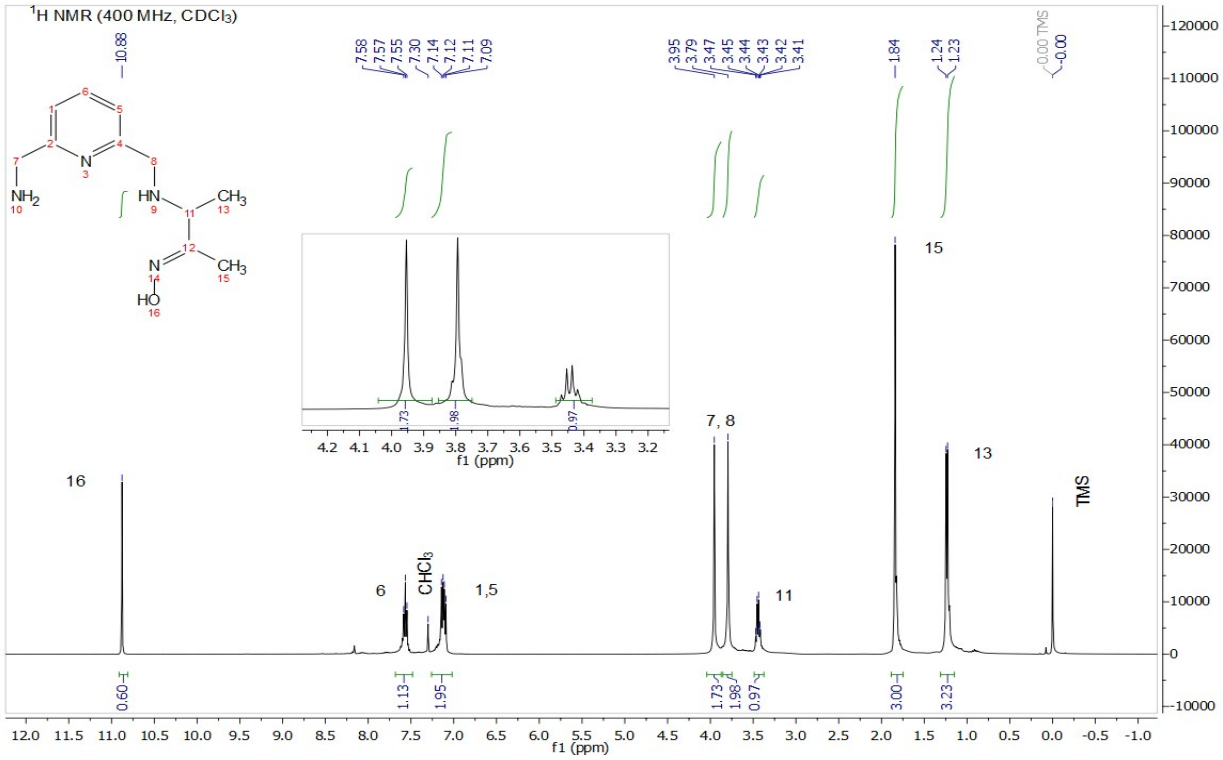

Fig 37S. ^{1}H-NMR spectra of **L3** in $CDCl_3$

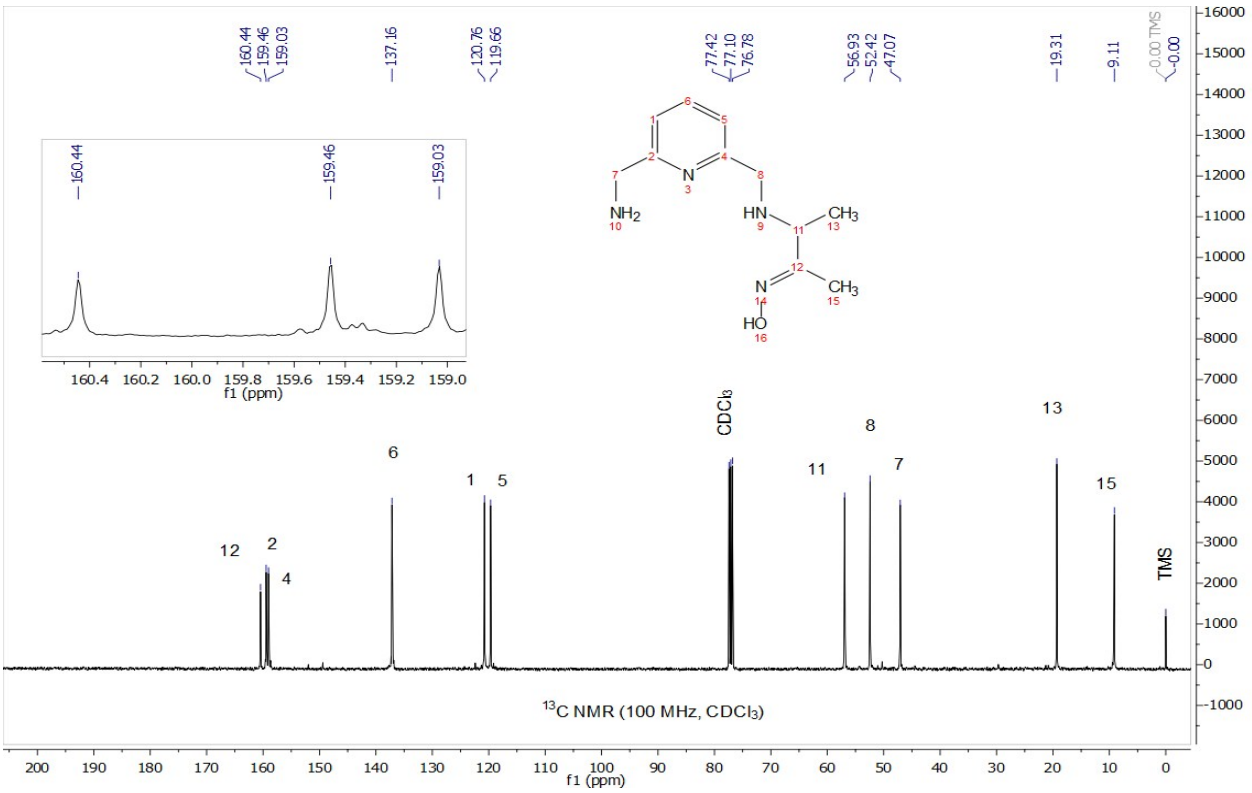

Fig 38S. ^{13}C-NMR spectra of **L3** in $CDCl_3$

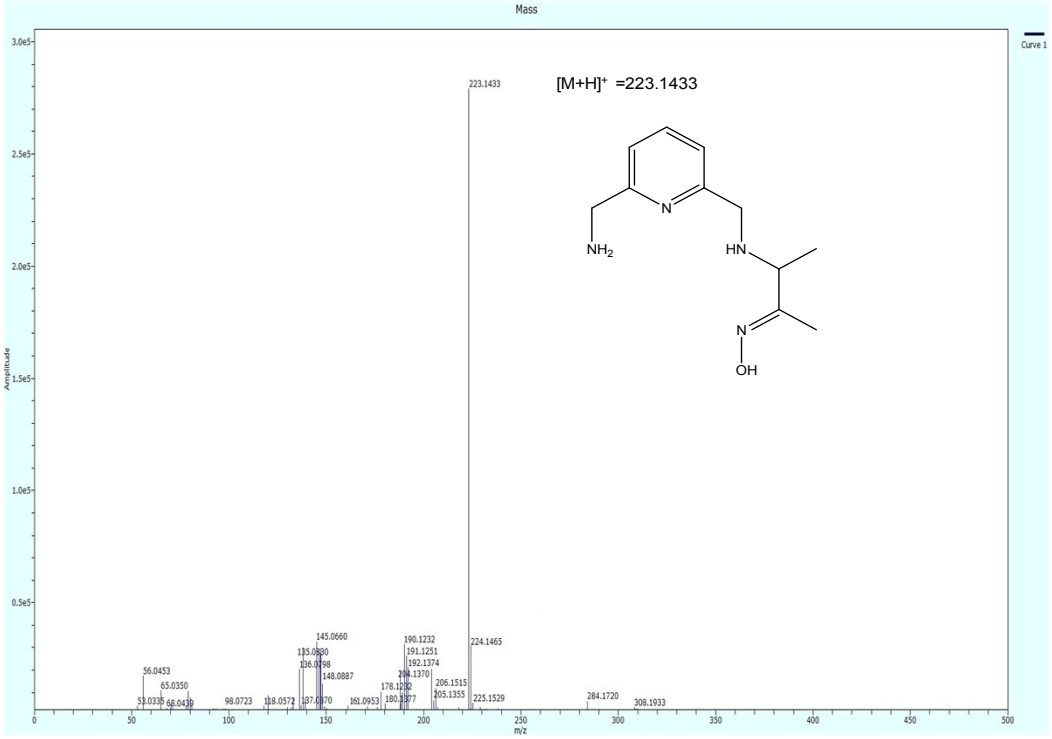

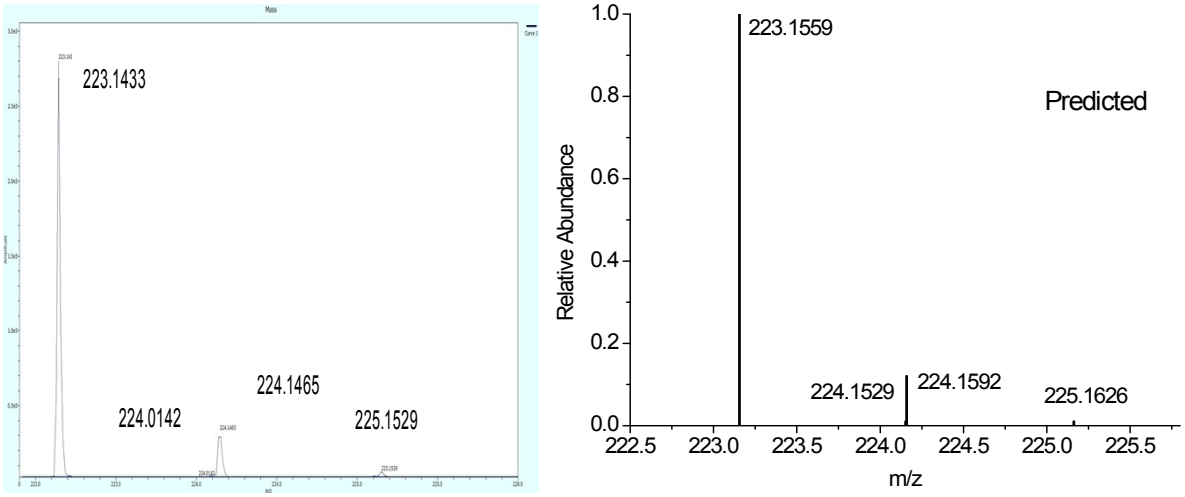

Fig 39S. APCI-mass spectrum (positive mode) of **L3.** High resolution $[M+H]^+$ 223.1433 and comparison of experimental *vs* calculated values.

Table S1. Crystal data and structure refinement for $[Cd(H\mathbf{L4})_2(NO_3)]NO_3$.

Compound	$[Cd(H\mathbf{L4})_2(NO_3)]NO_3$
Empirical formula	$C_{20}\ H_{30}\ Cd\ N_8\ O_8$
Formula weight	622.92
Temperature	130(2) K
Wavelength	0.71073 Å
Crystal system	Orthorhombic
Space group	P 21 21 21
Unit cell dimensions	a = 11.2439(7) Å
	b = 13.6597(8) Å
	c = 16.4470(12) Å
Volume	2526.1(3) $Å^3$
Z	4
Density (calculated)	1.638 Mg/m^3
Absorption coefficient	0.926 mm^{-1}
F(000)	1272
Crystal size	0.340 x 0.320 x 0.200 mm^3
Theta range for data collection	3.490 to 29.564°.
Index ranges	-15<=h<=10, -18<=k<=12, -20<=l<=11
Reflections collected	8710
Independent reflections	5445 [R(int) = 0.0304]
Completeness to theta = 25.242°	99.6 %
Absorption correction	Analytical
Max. and min. transmission	0.860 and 0.797
Refinement method	Full-matrix least-squares on F^2
Data / restraints / parameters	5445 / 4 / 351
Goodness-of-fit on F^2	1.029
Final R indices [I>2sigma(I)]	R1 = 0.0314, wR2 = 0.0615
R indices (all data)	R1 = 0.0358, wR2 = 0.0647
Absolute structure parameter	-0.02(3)
Largest diff. peak and hole	0.770 and -0.722 $e.Å^{-3}$

Table S2. Atomic coordinates (x 10^4) and equivalent isotropic displacement parameters ($Å^2$x 10^3) for Cd(H**L4**)$_2$(NO_3)$_2$. U(eq) is defined as one third of the trace of the orthogonalized U^{ij} tensor.

	x	y	z	U(eq)
C(1)	897(4)	5337(3)	3307(3)	21(1)
C(2)	786(4)	4353(3)	3506(3)	28(1)
C(3)	1776(4)	3845(3)	3729(3)	27(1)
C(4)	2856(4)	4322(3)	3747(3)	19(1)
C(5)	2915(3)	5307(3)	3556(2)	16(1)
C(6)	4052(4)	5862(3)	3651(3)	19(1)
C(7)	4947(3)	7462(3)	3442(3)	16(1)
C(8)	4214(4)	8102(3)	3989(3)	18(1)
C(9)	5533(4)	8073(3)	2776(3)	22(1)
C(10)	4835(4)	8786(3)	4562(3)	25(1)
C(11)	2613(3)	9676(3)	2518(2)	19(1)
C(12)	2616(3)	10569(3)	2136(3)	19(1)
C(13)	2568(4)	10601(3)	1301(3)	21(1)
C(14)	2553(3)	9733(3)	871(3)	17(1)
C(15)	2557(3)	8851(3)	1297(2)	14(1)
C(16)	2498(4)	7919(3)	820(2)	20(1)
C(17)	1903(4)	6227(3)	969(3)	18(1)
C(18)	659(4)	6344(3)	1292(3)	16(1)
C(19)	2403(4)	5220(3)	1183(3)	25(1)
C(20)	-319(4)	5787(4)	888(3)	29(1)
Cd(1)	2295(1)	7313(1)	2702(1)	14(1)
N(1)	1941(3)	5803(3)	3323(2)	17(1)
N(2)	4217(3)	6675(3)	3077(2)	16(1)
N(3)	3087(3)	8055(3)	3923(2)	18(1)
N(4)	2569(3)	8819(2)	2106(2)	15(1)
N(5)	2679(3)	7010(2)	1287(2)	15(1)
N(6)	529(3)	6914(3)	1894(2)	18(1)
N(7)	-265(4)	8075(3)	3938(3)	26(1)
N(8)	5762(3)	6711(3)	1035(2)	24(1)
O(1)	2510(3)	8715(2)	4435(2)	24(1)
O(2)	-647(2)	6967(2)	2172(2)	22(1)
O(3)	410(3)	8115(3)	3327(2)	30(1)
O(4)	-1302(3)	7808(3)	3858(2)	42(1)
O(5)	144(3)	8325(3)	4613(2)	35(1)
O(6)	6854(3)	6638(3)	1058(2)	40(1)
O(7)	5125(3)	6104(2)	1422(2)	27(1)
O(8)	5288(3)	7384(3)	645(2)	37(1)

Table S3. Bond lengths [Å] and angles [°] for $[Cd(H\mathbf{L4})_2(NO_3)]NO_3$.

C(1)-N(1)	1.335(5)
C(1)-C(2)	1.389(6)
C(1)-H(1)	0.9500
C(2)-C(3)	1.362(6)
C(2)-H(2)	0.9500
C(3)-C(4)	1.379(6)
C(3)-H(3)	0.9500
C(4)-C(5)	1.384(6)
C(4)-H(4)	0.9500
C(5)-N(1)	1.344(5)
C(5)-C(6)	1.494(6)
C(6)-N(2)	1.470(6)
C(6)-H(6A)	0.9900
C(6)-H(6B)	0.9900
C(7)-N(2)	1.481(5)
C(7)-C(8)	1.500(6)
C(7)-C(9)	1.527(6)
C(7)-H(7)	1.0000
C(8)-N(3)	1.273(5)
C(8)-C(10)	1.500(6)
C(9)-H(9A)	0.9800
C(9)-H(9B)	0.9800
C(9)-H(9C)	0.9800
C(10)-H(10A)	0.9800
C(10)-H(10B)	0.9800
C(10)-H(10C)	0.9800
C(11)-N(4)	1.353(5)
C(11)-C(12)	1.371(5)
C(11)-H(11)	0.9500
C(12)-C(13)	1.375(6)
C(12)-H(12)	0.9500
C(13)-C(14)	1.381(6)
C(13)-H(13)	0.9500
C(14)-C(15)	1.394(6)
C(14)-H(14)	0.9500
C(15)-N(4)	1.332(5)
C(15)-C(16)	1.497(6)
C(16)-N(5)	1.474(5)
C(16)-H(16A)	0.9900
C(16)-H(16B)	0.9900
C(17)-N(5)	1.475(5)
C(17)-C(18)	1.505(6)
C(17)-C(19)	1.527(6)
C(17)-H(17)	1.0000
C(18)-N(6)	1.267(6)
C(18)-C(20)	1.494(6)
C(19)-H(19A)	0.9800
C(19)-H(19B)	0.9800
C(19)-H(19C)	0.9800
C(20)-H(20A)	0.9800
C(20)-H(20B)	0.9800
C(20)-H(20C)	0.9800

Cd(1)-N(4)	2.300(3)
Cd(1)-N(1)	2.336(4)
Cd(1)-N(5)	2.403(3)
Cd(1)-N(2)	2.410(3)
Cd(1)-N(3)	2.421(4)
Cd(1)-N(6)	2.450(3)
Cd(1)-O(3)	2.598(3)
N(2)-H(2F)	0.92(2)
N(3)-O(1)	1.395(4)
N(5)-H(5F)	0.93(2)
N(6)-O(2)	1.401(4)
N(7)-O(4)	1.228(5)
N(7)-O(5)	1.249(5)
N(7)-O(3)	1.261(5)
N(8)-O(6)	1.232(4)
N(8)-O(8)	1.242(5)
N(8)-O(7)	1.266(5)
O(1)-H(1D)	0.84(2)
O(2)-H(2D)	0.84(2)
N(1)-C(1)-C(2)	122.4(4)
N(1)-C(1)-H(1)	118.8
C(2)-C(1)-H(1)	118.8
C(3)-C(2)-C(1)	118.9(4)
C(3)-C(2)-H(2)	120.6
C(1)-C(2)-H(2)	120.6
C(2)-C(3)-C(4)	119.0(4)
C(2)-C(3)-H(3)	120.5
C(4)-C(3)-H(3)	120.5
C(3)-C(4)-C(5)	119.8(4)
C(3)-C(4)-H(4)	120.1
C(5)-C(4)-H(4)	120.1
N(1)-C(5)-C(4)	121.1(4)
N(1)-C(5)-C(6)	118.2(4)
C(4)-C(5)-C(6)	120.7(4)
N(2)-C(6)-C(5)	115.1(4)
N(2)-C(6)-H(6A)	108.5
C(5)-C(6)-H(6A)	108.5
N(2)-C(6)-H(6B)	108.5
C(5)-C(6)-H(6B)	108.5
H(6A)-C(6)-H(6B)	107.5
N(2)-C(7)-C(8)	111.2(3)
N(2)-C(7)-C(9)	110.2(3)
C(8)-C(7)-C(9)	110.4(3)
N(2)-C(7)-H(7)	108.3
C(8)-C(7)-H(7)	108.3
C(9)-C(7)-H(7)	108.3
N(3)-C(8)-C(10)	123.2(4)
N(3)-C(8)-C(7)	117.8(4)
C(10)-C(8)-C(7)	118.9(4)
C(7)-C(9)-H(9A)	109.5
C(7)-C(9)-H(9B)	109.5

H(9A)-C(9)-H(9B)	109.5
C(7)-C(9)-H(9C)	109.5
H(9A)-C(9)-H(9C)	109.5
H(9B)-C(9)-H(9C)	109.5
C(8)-C(10)-H(10A)	109.5
C(8)-C(10)-H(10B)	109.5
H(10A)-C(10)-H(10B)	109.5
C(8)-C(10)-H(10C)	109.5
H(10A)-C(10)-H(10C)	109.5
H(10B)-C(10)-H(10C)	109.5
N(4)-C(11)-C(12)	122.7(4)
N(4)-C(11)-H(11)	118.6
C(12)-C(11)-H(11)	118.6
C(11)-C(12)-C(13)	119.1(4)
C(11)-C(12)-H(12)	120.5
C(13)-C(12)-H(12)	120.5
C(12)-C(13)-C(14)	118.9(4)
C(12)-C(13)-H(13)	120.5
C(14)-C(13)-H(13)	120.5
C(13)-C(14)-C(15)	119.0(4)
C(13)-C(14)-H(14)	120.5
C(15)-C(14)-H(14)	120.5
N(4)-C(15)-C(14)	122.0(4)
N(4)-C(15)-C(16)	119.8(3)
C(14)-C(15)-C(16)	118.1(4)
N(5)-C(16)-C(15)	115.9(3)
N(5)-C(16)-H(16A)	108.3
C(15)-C(16)-H(16A)	108.3
N(5)-C(16)-H(16B)	108.3
C(15)-C(16)-H(16B)	108.3
H(16A)-C(16)-H(16B)	107.4
N(5)-C(17)-C(18)	110.4(3)
N(5)-C(17)-C(19)	110.7(3)
C(18)-C(17)-C(19)	110.9(4)
N(5)-C(17)-H(17)	108.2
C(18)-C(17)-H(17)	108.2
C(19)-C(17)-H(17)	108.2
N(6)-C(18)-C(20)	125.1(4)
N(6)-C(18)-C(17)	116.6(4)
C(20)-C(18)-C(17)	118.3(4)
C(17)-C(19)-H(19A)	109.5
C(17)-C(19)-H(19B)	109.5
H(19A)-C(19)-H(19B)	109.5
C(17)-C(19)-H(19C)	109.5
H(19A)-C(19)-H(19C)	109.5
H(19B)-C(19)-H(19C)	109.5
C(18)-C(20)-H(20A)	109.5
C(18)-C(20)-H(20B)	109.5
H(20A)-C(20)-H(20B)	109.5
C(18)-C(20)-H(20C)	109.5
H(20A)-C(20)-H(20C)	109.5
H(20B)-C(20)-H(20C)	109.5
N(4)-Cd(1)-N(1)	177.70(12)
N(4)-Cd(1)-N(5)	73.60(11)
N(1)-Cd(1)-N(5)	107.62(12)
N(4)-Cd(1)-N(2)	108.20(11)
N(1)-Cd(1)-N(2)	73.83(11)
N(5)-Cd(1)-N(2)	91.39(12)
N(4)-Cd(1)-N(3)	85.95(12)
N(1)-Cd(1)-N(3)	93.96(12)
N(5)-Cd(1)-N(3)	144.08(12)
N(2)-Cd(1)-N(3)	66.97(12)
N(4)-Cd(1)-N(6)	94.40(11)
N(1)-Cd(1)-N(6)	84.44(12)
N(5)-Cd(1)-N(6)	65.30(12)
N(2)-Cd(1)-N(6)	141.70(12)
N(3)-Cd(1)-N(6)	147.32(11)
N(4)-Cd(1)-O(3)	84.28(11)
N(1)-Cd(1)-O(3)	93.45(12)
N(5)-Cd(1)-O(3)	127.09(11)
N(2)-Cd(1)-O(3)	141.47(12)
N(3)-Cd(1)-O(3)	78.15(11)
N(6)-Cd(1)-O(3)	69.39(11)
C(1)-N(1)-C(5)	118.8(4)
C(1)-N(1)-Cd(1)	124.2(3)
C(5)-N(1)-Cd(1)	115.5(3)
C(6)-N(2)-C(7)	110.9(3)
C(6)-N(2)-Cd(1)	108.9(2)
C(7)-N(2)-Cd(1)	109.8(2)
C(6)-N(2)-H(2F)	109(3)
C(7)-N(2)-H(2F)	108(3)
Cd(1)-N(2)-H(2F)	111(3)
C(8)-N(3)-O(1)	112.3(3)
C(8)-N(3)-Cd(1)	117.2(3)
O(1)-N(3)-Cd(1)	126.9(2)
C(15)-N(4)-C(11)	118.2(3)
C(15)-N(4)-Cd(1)	116.9(2)
C(11)-N(4)-Cd(1)	124.5(3)
C(16)-N(5)-C(17)	110.2(3)
C(16)-N(5)-Cd(1)	109.6(2)
C(17)-N(5)-Cd(1)	111.2(3)
C(16)-N(5)-H(5F)	108(3)
C(17)-N(5)-H(5F)	106(3)
Cd(1)-N(5)-H(5F)	112(3)
C(18)-N(6)-O(2)	113.3(3)
C(18)-N(6)-Cd(1)	117.8(3)
O(2)-N(6)-Cd(1)	125.2(2)
O(4)-N(7)-O(5)	121.8(4)
O(4)-N(7)-O(3)	119.9(4)
O(5)-N(7)-O(3)	118.3(4)
O(6)-N(8)-O(8)	120.2(4)
O(6)-N(8)-O(7)	119.7(4)
O(8)-N(8)-O(7)	120.0(3)
N(3)-O(1)-H(1D)	108(4)
N(6)-O(2)-H(2D)	100(3)
N(7)-O(3)-Cd(1)	142.1(3)

Table S4. Hydrogen bonds for $[Cd(H\mathbf{L4})_2(NO_3)]NO_3$ [Å and °].

D-H...A	d(D-H)	d(H...A)	d(D...A)	<(DHA)
N(2)-H(2F)...O(7)	0.92(2)	2.11(3)	3.010(5)	164(4)
N(5)-H(5F)...N(8)	0.93(2)	2.62(3)	3.515(5)	164(4)
N(5)-H(5F)...O(7)	0.93(2)	2.14(3)	3.023(5)	159(4)
N(5)-H(5F)...O(8)	0.93(2)	2.39(3)	3.159(5)	140(4)
O(1)-H(1D)...N(7)	0.84(2)	2.52(3)	3.342(5)	164(5)
O(1)-H(1D)...O(3)	0.84(2)	2.43(4)	3.092(4)	136(5)
O(1)-H(1D)...O(5)	0.84(2)	1.90(3)	2.729(5)	166(5)
O(2)-H(2D)...N(7)	0.84(2)	2.50(3)	3.304(5)	160(4)
O(2)-H(2D)...O(3)	0.84(2)	1.97(3)	2.736(5)	152(4)
O(2)-H(2D)...O(4)	0.84(2)	2.39(4)	3.090(5)	142(4)

Symmetry transformations used to generate equivalent atoms:

#1 -x+1,y-1/2,-z+1/2 #2 x+1/2,-y+3/2,-z+1 #3 -x+1,y+1/2,-z+1/2

#4 -x,y+1/2,-z+1/2 #5 -x+1/2,-y+2,z-1/2 #6 x-1/2,-y+3/2,-z

#7 x-1,y,z

References

1. A. E. Martell, R. M. Smith, A. E. Martell and R. M. Smith, in *Critical Stability Constants*, Springer US, 1982, 132–200.
2. R. D. Hancock and A. E. Martell, *Supramol. Chem.*, 1996, **6**, 401–407.
3. D. Buist, N. J. Williams, J. H. Reibenspies and R. D. Hancock, *Inorg. Chem.*, 2010, **49**, 5033–5039.
4. Y. H. Chiu and J. W. Canary, *Inorg. Chem.*, 2003, **42**, 5107–5116.
5. S. Abada, A. Lecointre, M. Elhabiri and L. J. Charbonnière, *Dalt. Trans.*, 2010, **39**, 9055–9062